EFFECT OF ION-CLUSTERING AND DIANION FORMATION ON THE RATE OF REACTION OF ANTHRACENIDE RADICAL ANION WITH ETHANOL IN THF

Thesis for the Degree of Ph. D.
MICHIGAN STATE UNIVERSITY
LE DINH LONG
1973



This is to certify that the

thesis entitled

ON THE RATE OF REACTION OF ANTHRACENIDE RADICAL ANION WITH ETHANOL IN THF presented by

Le Dinh Long

has been accepted towards fulfillment of the requirements for

Ph.D. degree in Chemistry

Major professor

O-7639

BINDING BY
HOAG & SONS'
HOAG & SONS'
LIBRARY BINDERS
SPRINEPORT, MICHIGAN

The problem of the problem of contrarge of contrarge of contrarge of contrarge anthrace with the problem of the

2

Matio [ROH]/

anthracene.

'dlanion meg

ķ.

ABSTRACT

ON THE RATE OF REACTION OF ANTHRACENIDE
RADICAL ANION WITH ETHANOL IN THE

Ву

Le Dinh Long

The protonation of potassium anthracenide (K⁺An⁻), by ethanol in tetrahydrofuran (THF), was studied over a wide range of concentrations of ethanol and free anthracene.

A rapid scanning stopped-flow apparatus was used in the study.

The anthracenide anion was produced by the reduction of anthracene with potassium metal in THF.

The protonation rate was largely second-order in the absorbance, thus revealing the existence of intermediate steps prior to the protonation step. At low alcohol concentrations, the pseudo second-order constant depended upon the ratio [ROH]/[An], where [An] denotes the concentration of free anthracene. These results are consistent with the following "dianion mechanism":

$$2 (An^{-}, K^{+}) \xrightarrow{k_{+}} (An^{-}, 2K^{+}) + An$$
 $(An^{-}, 2K^{+}) + ROH \xrightarrow{k_{1}} K^{+}AnH^{-} + K^{+}RO^{-}$
 $K^{+}AnH^{-} + ROH \xrightarrow{fast} AnH_{2} + K^{+}RO^{-}$

At high condincreased was [An]. This

cluster inte

and ion-clus

2(An⁺,

(An⁼,2)

(An⁺,K

K⁺AnH

an attractive cation solve might be pro-

system. Thi

supported by

the alcohol

A prei

crown-6 (cr

Crown elimi

slow first-

provides st

Pathway reg

At high concentrations of alcohol, the rate of protonation increased with [ROH], but did not depend significantly on [An]. This suggested the participation of a quadruple ion-cluster intermediate as the protonated species. A "dianion and ion-cluster mechanism" was then proposed:

$$2 (\operatorname{An}^{-}, \operatorname{K}^{+}) \xrightarrow{\operatorname{K}_{Q}} (\operatorname{An}^{-}, \operatorname{K}^{+})_{2} \xrightarrow{\operatorname{K}_{+}^{+}} (\operatorname{An}^{=}, 2\operatorname{K}^{+}) + \operatorname{An}$$

$$(\operatorname{An}^{=}, 2\operatorname{K}^{+})_{2} + \operatorname{ROH} \xrightarrow{\operatorname{K}_{2}^{+}} \operatorname{K}^{+} \operatorname{AnH}^{-} + \operatorname{K}^{+} \operatorname{RO}^{-}$$

$$(\operatorname{An}^{-}, \operatorname{K}^{+})_{2} + \operatorname{ROH} \xrightarrow{\operatorname{K}_{2}^{+}} \operatorname{K}^{+} \operatorname{AnH}^{-} + \operatorname{K}^{+} \operatorname{RO}^{-} + \operatorname{An}$$

$$\operatorname{K}^{+} \operatorname{AnH}^{-} + \operatorname{ROH} \xrightarrow{\operatorname{fast}} \operatorname{AnH}_{2}^{+} \operatorname{K}^{+} \operatorname{RO}^{-}$$

An attractive alternate mechanism was also proposed: the "cation solvation mechanism", in which the intermediate species might be protonated by K*.ROH already present in the aromatic system. This "intra-complex" protonation scheme was further supported by the apparent insensitivity of the protonation rate at relatively high values of [ROH] toward the nature of the alcohol used.

A preliminary study of the effect of dicyclohexyl-18-crown-6 (crown) on the rate of protonation was also undertaken. Crown eliminated the second-order component, leaving only a slow first-order contribution to the rate. The effect of crown provides strong evidence that the second-order protonation pathway requires contact ion-pair formation.

sistent wing chargedianion (contact in the contact in the contact

Thes

These results and those of other investigators are consistent with a decrease in the protonation rate with decreasing charge localization in the aromatic system in the order: dianion $(An^{\pm}, 2K^{\pm})$ > quadruple ion-cluster $(An^{\pm}, K^{\pm})_2$ contact ion-pair (An^{\pm}, K^{\pm}) > solvent-separated ion pair $(An^{\pm} | K^{\pm})$ > free or solvent solvated ion (An^{\pm}) .

ON THE RATE OF REACTION OF ANTHRACENIDE RADICAL ANION WITH ETHANOL IN THF

Ву

Le Dinh Long

A THESIS

Submitted to
Michigan State University
in partial fulfillment of the requirements
for the degree of

DOCTOR OF PHILOSOPHY

Department of Chemistry

Garan S

To:

My Parents and Ngoc-Xuân

The autorios extended by the autorios extended

for Interna

ACKNOWLEDGEMENTS

The author wishes to express his sincere appreciation to Professor James L. Dye whose invaluable guidance, assistance and encouragement greatly contributed to the completion of this work.

He also wishes to thank Mr. Joseph M. Ceraso, a special friend, for his untiring help during the tedious hours of kinetics experiments as well as data analysis.

The author is indebted to Mssrs. Frederick J. Tehan,
Richard B. Coolen, Mei-Tak Lok, Nicholas Papadakis and Dr.
Marc G. DeBacker for their valuable suggestions.

Finally, financial support from the United States Agency for International Development is gratefully acknowledged.

I. INTRO

II. HISTO

2.

2.2

III. EXPERII

3.1. 3.2.

TABLE OF CONTENTS

	Page
I. INTRODUCTION	1
II. HISTORICAL	4
2.1Early Studies	4
Alkali Metals	4
2.1.2Studies of Optical Spectra	5
2.1.3Electrochemical Studies	6
2.1.4E.S.R. Studies	7
2.1.5Ion-pairing Studies	9
2.1.5.1Evidence for a Dissociative	_
Equilibrium	10
2.1.5.2-Evidence for a Non-dissoci-	
ative Equilibrium	12
2.1.5.3Other Equilibria	14
2.1.5.4Conclusions Regarding Ion-	
pairing	15
2.2Kinetics Studies	15
2.2.1The Mechanism of Paul, Lipkin and	
Weissman	15
2.2.2Kinetics Studies in Ammonia	16
2.2.3Pulse-radiolysis Studies	21
2.2.4Kinetics Study Using ESR and Polar-	
ography	24
2.2.5Combined Polarography-ESR-UV Absorp-	
tion Spectroscopy Studies	25
2.2.6Kinetics Studies Using Polarography	
and Stopped-flow	27
2.2.7Stopped-flow Studies	28
2.2.7.1The Work of Minnich	28
2.2.7.2-The Studies of Bank and	
Bockrath	30
2.2.7.3The Studies of Szwarc and	30
Co-workers	32
III. EXPERIMENTAL	36
3.1Vacuum Techniques	36
3 2-Cleaning Techniques	36

TABLE C

•

3

ر

W. SURVE

٦,

V. RESUL

5.

5.2

5.3 5.4

REFERENCE

TABLE OF CONTENTSContinued	Page
2 2 Durification Machaiana	27
3.3Purification Techniques	37
3.3.1Tetrahydrofuran	
3.3.2Alcohols	
3.3.3Alkali metals	39
3.3.4Anthracene and Crown	39
3.3.5Helium	39
3.4Preparation	40
3.4.1Pre-rinsing Techniques	40
3.4.2Anthracene and Crown Solutions	
3.4.3Alcohol Solutions	42
3.4.4Anion Solutions	42
3.5The Stopped-flow Experiment	
3.5.1General	
3.5.2The Stopped-flow Apparatus	45
3.5.3Calibration of the Stopped-flow	
System	49
3.5.4Operations	51
3.5.5Data Acquisition	
3.5.6Data Analysis	
3.5.6.1General	58
3.5.6.2Program PUNDAT	63
3.5.6.3Program KINFIT	64
IV. SURVEY AND TREATMENT OF THE DATA	65
A. 1. C. marris at 1. Diana and a second at 1. a. Data	6.5
4.1Survey and Discussion of the Data	65
4.2Data Treatment	68
V. RESULTS AND CONCLUSIONS	75
5.1Results	75
5.1.1Inapplicable Mechanisms	75
	78
5.1.2Effect of Crown	
5.1.3Proposed Mechanisms	78
5.1.3.1Dianion and Ion-cluster	
Mechanism	81
5.1.3.2Cation Solvation Mechanism .	85
5.2Discussion	95
5.2.1Comparison of the Two Proposed	
Mechanisms	95
5.2.2Discrepancies Between Some of	
Minnich's Results and Those of Bank	
and Bockrath	98
	99
5.3Summary	
5.4Conclusion and Suggestions for Further Work.	100
DEEEDENCEC	103

III. Obse Con: THF Eth:

IV. Calo

V. Pseu tion Minn

LIST OF TABLES

TABLE	Ε	Page
ı.	List of Experiments	66
II.	List of Minnich's Experiments Re-analyzed by the Author (2K+An + 2ROH THF AnH 2 + An + 2K+RO-)	69
III.	Observed and Calculated Pseudo Second-order Rate Constants for the Reaction of K ⁺ An ⁻ with EtOH in THF and Pseudo First-order Contribution at High Ethanol Concentrations (from this study)	86
IV.	Calculated Constants from Equation 70	89
v.	Pseudo Second-order Rate Constants for the Reaction 2K+An + 2ROH THF AnH + 2K+OR + An (from Minnich's re-analyzed data)	96

FIGURE

- 1. Spec
- 2. Vesse or RC
- 3. Schem
- 4. Syrin
- 5. Four-
- 6. Absor
- 7. Decay EtOH
- 8. Block
- 9. Decay 0.0052
- 10. Decay 0.090
- 11. Block
- 12. Parall to the x 10-2
- 13. Log-lo
- 14. Log-lo and (b EtOH i
- li. Pseudo (exces

LIST OF FIGURES

FIGU:	RE	Page
1.	Special set-up for pre-rinsing technique	41
2.	Vessels used in the preparation of: (a) An, crown or ROH solutions (b) K+An solutions	43
3.	Schematic diagram of the stopped-flow apparatus	46
4.	Syringe used in the stopped-flow system	48
5.	Four-jet mixing cell	50
6.	Absorbance vs C/C of the solutions of KMnO4 in H2O	52
7.	Decay of spectrum of K ⁺ An ⁻ during reaction with EtOH in THF	54
8.	Block diagram of the data-acquisition system	55
9.	Decay of the 720 nm peak of K ⁺ An ⁺ after mixing with 0.0052 M EtOH in THF (scanning technique)	59
10.	Decay of the 720 nm peak of K ⁺ An ⁻ after mixing with 0.090 M EtOH in THF (fixed wavelength technique)	60
11.	Block diagram of the analysis system	62
12.	Parallel first- and second-order kinetics applied to the reaction K An + EtOH in THF ([EtOH] = 8.9 x 10 ⁻² M)	72
13.	Log-log plot of k_{ps} (second-order) vs [EtOH] for the reaction of K+An with EtOH in THF	76
14.	Log-log plot of k_{ps} (second-order) \underline{vs} (a) [EtOH] and (b) [EtOH]/[An], for the reaction of $K^{\dagger}An^{\dagger}$ with EtOH in THF	77
15.	Pseudo first-order plot for the reaction of K ⁺ An ⁻ + (excess crown) with EtOH in THF	79

LIS

FIG

16.

17.

18.

19.

LIST OF FIGURES--Continued

FIGURE	Page
16. C/C vs time for the reaction: 2K ⁺ An ⁻ + 2EtOH THFO AnH ₂ + An + 2K ⁺ EtO	80
17. Log-log plot of $f_{obs} \stackrel{vs}{=} f_{calc} \dots \dots$	88
18. C/C vs time for the reaction of K An with EtOH in THF at three different values of [EtOH]	90
19. Log-log plot of kps (second-order) vs [ROH]/[An] for the reaction of K+An with i-PrOH, H2O, t-BuOH, MeOH, EtOH in THF	93

form a sign i aromat odd nw

we wil

radica

A. Dethod

a

b)

c)

Ar strongl They re

referre

Propert

The

I. INTRODUCTION

An aromatic molecule Ar may accept an extra electron to form a new species which we will denote by Ar. The negative sign in this symbol represents the negative charge of the aromatic ion; the dot shows that the new species possesses an odd number of electrons, and thus, a radical nature. Hence, we will reserve for the new species Ar. the term aromatic radical anion.

Aromatic radical anions are formed by three common methods as follows:

- a) reduction of the parent aromatic hydrocarbon via reaction with alkali metals;
- b) electrolytic reduction of the aromatic molecule;
- c) reduction by solvated electrons produced by pulseradiolysis.

Aromatic radical anions are paramagnetic, conducting and strongly colored species. They are good reducing agents.

They react with air and with proton donors. (The reader is referred to the Historical section for more details on the properties of Ar and for references.)

The protonation of aromatic radical anions by alcohols has the following stoichiometry:

wher

cule is f

et a

in m

beha:

tech:

anthi

fura:

tion.

exist

tonat

the c

over

and R

flow

of so

alcoho

With t

(Pe⁼,2

$$2Ar^{+} + 2ROH \longrightarrow ArH_{2} + Ar + 2RO^{-}$$

where ArH, is the dihydroproduct of the parent aromatic molecule Ar. Paul, Lipkin and Weissman assumed that this reaction is first-order in Ar . Pulse-radiolysis studies by Dorfman et al. of a series of aromatic compounds in pure alcohols and in mixtures of ethanol and other solvents did show first-order behavior in Ar . However, when Minnich used the stopped-flow technique to study the protonation of sodium and potassium anthracenide with various alcohols and water in tetrahydrofuran (THF), he found that the reaction was second-order in the Ar concentration and of low order in the ROH concentra-This second-order behavior was consistent with the existence of a quadruple ion-cluster (Ar,M,), as the protonated intermediate species. However, Minnich did not vary the concentrations of the various alcohols and the anthracene over wide enough ranges to test completely the effect of An and ROH concentration on the protonation rate. At about the same time, Levin, Sutphen and Szwarc, also using the stoppedflow technique, observed a second-order decay of the absorbance of sodium perylenide (Na Pe) in its reaction with various alcohols in THF. They also found the reaction to be of inverse first-order in the perylene (Pe) concentration, consistent with the protonation of the ion-paired perylene dianion (Pe , 2Na) as the intermediate species.

ha: wi

wor

rad s;;s

wit:

tra

beha

quad hold

posed

up bj ïs.

: ರ್ಷಾ of io:

Will f

furthe

In order to investigate further the second-order behavior in the protonation reaction of aromatic radical anions with alcohols in ethereal solvents, we decided to extend the work of Minnich. However, instead of using various aromatic radical anions and various alcohols, we chose only a single system for study. The reaction of potassium anthracenide with ethanol in THF was studied over a wide range of concentrations of EtOH and An. We found the same second-order behavior as did Minnich. But we also found that neither the quadruple ion-cluster nor the anthracene dianion mechanism holds over a wide concentration range of EtOH and An.

At the end of this thesis, several mechanisms are proposed which are consistent with our experimental data, backed up by some of Minnich's data which have been re-analyzed by us. We also used dicyclohexyl-18-crown-6 (crown), a good complexing agent for alkali metal cations, to test the effect of ion-pairing on the protonation rate. Finally, the reader will find at the very end of this thesis some suggestions for further work in this unpredictable but fascinating field.

wil

of bec

of

:ec

the

rec

Piit

2.1

cari

sing

àt.d

in d

ites

dist

late

II. HISTORICAL

The Historical section of this rapidly expanding subject will be divided into two main parts: early studies and studies of kinetics. The first part deals with the general properties of the aromatic radical anions, with emphasis on ion-pairing because, as will be shown later, ion-pairing drastically affects the protonation rate. The second part presents all of the studies which have dealt with protonation kinetics, from the early studies of Paul, Lipkin and Weissman to the most recent paper of Szwarc and co-workers which is about to be published.

2.1--Early Studies

2.1.1--Production of Ar via Reduction with Alkali Metals

It has been known for a long time that aromatic hydrocarbons can react with alkali metals. The first comprehensive study on such a reaction can be attributed to Schlenk and co-workers (1) who, in 1914, mixed sodium and anthracene in diethyl ether solutions. They reported the formation of two distinct compounds: a one-to-one and a two-to-one adduct (respectively sodium anthracenide and disodium anthracene).

Later, Scott, Walker and Hansley (2) found that the reaction

o**£**

us: The

Ine

c£

2.1,

the Prod

arom

exan

sodiy both

teact

of aromatic hydrocarbons with sodium is greatly facilitated by using dimethyl ether as the solvent in place of diethyl ether. The sodium naphthalenide solutions are dark green in color. These solutions are also electrically conducting. Two classes of reaction of sodium naphthalenide were reported:

- a) reversal of the reduction step by reaction with mercury, oxygen or benzyl chloride, in which the naphthalene is recovered unchanged;
- b) an irreversible reaction with water, alcohols and other proton donors, in which the naphthalene is reduced to dihydronaphthalene or its derivatives depending on the reagent used. This type of reaction was represented by the following equation: ${}^{\text{C}}_{10}{}^{\text{H}}_{8} \cdot {}^{\text{Na}}_{2} \cdot {}^{\text{C}}_{10}{}^{\text{H}}_{8} + {}^{\text{C}}_{10}{}^{\text{H}}_{8} + {}^{\text{C}}_{10}{}^{\text{H}}_{10} + {}^{\text{2NaR}}$ (1)

2.1.2--Studies of Optical Spectra

in which R is the conjugate base.

Paul, Lipkin and Weissman (3) studied the optical spectra, the stoichiometry and the electrical conductance of the products of the reaction of metallic sodium with various aromatic hydrocarbons in tetrahydrofuran (THF). All of these reaction products were reported to have deep colors; for example, green for sodium naphthalenide, brilliant blue for sodium anthracenide, etc. Studies of the optical spectra of both the mono- and di-anions of the products formed by the reaction of numerous aromatic hydrocarbons with Li, Na and K



in 1,2-dimethoxyethane (DME) and in THF were also reported (4,5). The polarizations of the electronic transitions were studied by Hoijtink et al. (6,7).

2.1.3--Electrochemical Studies

In addition to their production by reduction of the aromatic molecules by alkali metals, aromatic radical anions can be produced via electrochemical reduction of the parent aromatic compounds. The pioneering work of Laitinen and Wawzonek (8) showed that polarographic reductions of aromatic hydrocarbons (Ar) follow the scheme:

$$Ar + e^{-} \longrightarrow Ar^{-}$$
 (2a)

$$Ar^{-} + e^{-} \longrightarrow Ar^{-}$$
 (2b)

followed by:

$$Ar^{-} + 2H_{2}O \longrightarrow ArH_{2} + 2OH^{-}$$
 (2c)

since the experiments were conducted in dioxane-water mixtures. Later, Maccoll (9) and Hoijtink and Van Schooten (10) (using zero-order molecular orbital calculations) correlated the half-wave potentials $\varepsilon_{\frac{1}{2}}$ with the energies of the lowest unoccupied orbitals, E. They found a linear relationship between $\varepsilon_{\frac{1}{2}}$ and E. Hoijtink and Van Schooten (10) also noted another possible mechanism for the protonation of aromatic hydrocarbons as follows:

$$Ar + e^{-} \longrightarrow Ar^{-}$$
 (3a)

$$Ar^{-} + H_2O \longrightarrow ArH^{+} + OH^{-}$$
 (3b)

$$ArH^{\bullet} + e^{-} \longrightarrow ArH^{-}$$
 (3c)

$$ArH^- + H_2O \longrightarrow ArH_2 + OH^-$$
 (3d)

Also, polarographic studies with varying dioxane-water mixtures and with varying HI concentrations (11) showed one two-electron wave in the case of high water concentrations (or upon the addition of HI), and two one-electron waves for low concentrations of proton donors. These data indicated that high concentrations of proton donors favor step (3b) while step (2b) is favored at low concentrations. Finally, the species (ArH⁻) seems to protonate more readily than does the parent radical anion Ar⁻.

In later studies (12), the biphenylide anion (Biph*)

produced by the reaction of sodium with biphenyl was used to

reduce other aromatic compounds. Potentiometric titrations

showed that diamions could also be produced, but in two steps:

$$Biph^{\bullet} + Ar \longrightarrow Biph + Ar^{\bullet}$$
 (4a)

$$Biph^{-} + Ar^{-} \longrightarrow Biph + Ar^{-}$$
 (4b)

2.1.4--E.S.R. Studies

Aromatic radical anions (Ar*) are paramagnetic since they have an odd number of electrons. Thus one can use the sensitive electron spin resonance technique to study some of

their prop
from aroma
Early ESR
due to the
nuclei in
splits the
splitting
ing the od
ESR studie
ESR spectr
calculated
hyperfine
ty on the

Note tron dens which con

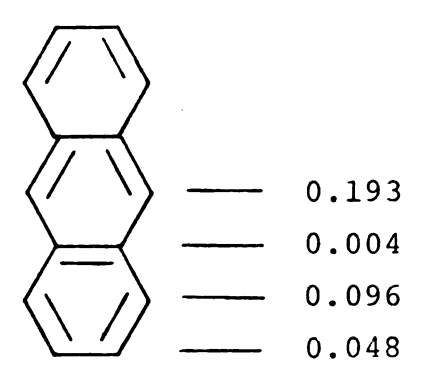
and calcul

anion the

Yet, the

their properties. On the other hand, the diamions formed from aromatic hydrocarbons are generally diamagnetic (13).

Early ESR studies of Ar^T (14,15) revealed hyperfine structure due to the interaction of the odd electron with the magnetic nuclei in the investigated species. Each magnetic nucleus splits the ESR signal, and for a given type of nucleus, the splitting constant is proportional to the probability of finding the odd electron at that nucleus. In one of their early ESR studies, DeBoer and Weissman (16) compared the observed ESR spectra of numerous aromatic radical anions with those calculated on the assumption of a linear relationship between hyperfine coupling constant with a proton and the π-spin density on the adjacent carbon. Good agreement between observed and calculated spectra was reported. For the anthracene monoanion the distribution of the spin densities is as follows:



Note that while certain positions are favored, the electron density is distributed over the entire aromatic system, which consequently makes the species very stable once formed. Yet, the extra electron can jump back and forth from one

aromatic molecule to another, as shown by Ward and Weissman (17). These authors observed a broadening of the ESR spectrum of naphthalenide (Nap*) when they added extra naphthalene (Nap) to the Nap* solutions. They concluded that the broadening resulted from the exchange reaction:

$$Nap + Nap$$
 \longrightarrow $Nap + Nap$ (5)

Second-order rate constants from 1×10^7 to 1×10^9 M⁻¹sec⁻¹ were reported, depending on the solvent and on the positive ion used.

ESR studies also reveal another interesting phenomenon; ion-pairing of the aromatic mono-anion species with cations.

2.1.5--Ion-pairing Studies

As described above, the ESR technique can reveal the hyperfine interactions of an aromatic radical anion. For example, the ESR hyperfine structure of a free naphthalene radical anion is due to the magnetic interaction of the odd electron with two sets, α and β , of four equivalent protons. These split the ESR signal into 25 lines. But the spectrum of the sodium naphthalenide ion-pair is more complex. The odd electron has a finite probability density at the $^{23}{\rm Na}$ nucleus. This nucleus has spin 3/2 so that each of the original 25 lines is split further into a quadruplet. Atherton and Weissman (18) reported this additional splitting of the spectrum of sodium naphthalenide in THF, and postulated the

existen

Na +

They als

sodium si

center of

cf about

position,

showed the

not adequate

ther stud

two or more

the variou

reported:

- a

M

A (:)

the foli

2.1.5.1--<u>E</u>-Condu

Fr broduc

that for p

existence of an ion-pairing equilibrium:

$$Na^{\dagger}Nap^{\dagger} \longrightarrow Na^{\dagger} + Nap^{\dagger}$$
 (6)

They also went further and suggested that the existence of the sodium splitting would require the Na⁺ion to lie above the center of either of the two benzene rings and at a distance of about 2.5 Å. If the Na⁺ion shifted from this equilibrium position, the splitting would decrease. Later experiments showed that this pioneering description of ion-pairing was not adequate to describe all of the phenomena which can occur. Other studies showed that aromatic radical anions can exhibit two or more forms of ion-pairing with equilibria connecting the various forms. Two general classes of equilibria were reported:

a dissociative equilibrium:

$$M^{\dagger}Ar^{\dagger} \longrightarrow M^{\dagger} + Ar^{\dagger}$$
 (7)

A non-dissociative equilibrium:

$$(M^{\dagger}Ar^{\dagger})_{a} \iff (M^{\dagger}Ar^{\dagger})_{b}$$
 (8)

In the following sections, we will give evidence for both classes of equilibria.

2.1.5.1--Evidence for a Dissociative Equilibrium

Conductance measurements (19) of the solutions of several Ar produced by reduction with alkali metals in THF showed that for potassium anthracenide (K An) the specific conductance

and then do behavior horses in solvent visible the res

and Li ant continues stantial s the optica absorption alkali cat

where An

into free ESR s

and small

Tethyl-te:

concentra the two s

dissocia+

extended clude all

Same sup

increased with temperature from -75°C to a maximum at 0°C and then decreased slightly from 0°C to 25°C. While the behavior below 0°C was interpreted as due to the normal increase in conductivity of the ions with a decrease in the solvent viscosity, the behavior above 0°C was postulated to be the result of a shift to the left of the equilibrium:

$$M^{\dagger}An^{\dagger} \longrightarrow M^{\dagger} + An^{\dagger}$$
 (9)

where An represents the anthracenide mono-anion. For Na and Li anthracenide solutions, the specific conductance continues to increase from -75°C to 25°C, indicating no substantial shift of equilibrium (9) to the left. Studies of the optical spectra of these same solutions showed that the absorption peaks occurred at higher energies for the smaller alkali cations. It seems that low temperatures, large anions and small cations enhance the dissociation of the ion-pairs into free ions.

methyl-tetrahydrofuran (MTHF) at low temperatures (20) showed a superposition of two distinct ESR spectra. Changes in anion concentrations led to changes in the relative intensities of the two spectra. These results indicated the existence of a dissociative equilibrium. When Dodson and Reddoch (21) extended the ESR study of the naphthalenide solutions to include all of the alkali metals in THF and DME, they found the same superposition of spectra at room temperature. In most

case spec

meit

woul

shif ±:he

radi

207.5

crea

2.1.

tru of p

Vari

ture

Peak Sinc

of a

e<u>li-</u>

it th

cases, they found the same concentration dependence of the ESR spectra. The spectrum of Li naphthalenide in DME showed neither metal splitting nor concentration dependence. This would be the case if the dissociative equilibrium (7) was shifted far to the right. Slates and Szwarc (22), by studying the conductance of the sodium salts of numerous aromatic radical anions in THF, were able to determine the dissociation constants of the respective ion pairs. These constants increased with the size of the anion.

2.1.5.2--Evidence for a Non-dissociative Equilibrium

Hogen-Esch and Smid (23) reported that the optical spectrum of sodium fluorenyl (Na⁺Fl⁺) in THF contained a number of peaks whose relative intensities varied reversibly with variations in the temperature. For example, when the temperature was changed from +25°C to -50°C, there was growth of a peak at 356 nm simultaneously with decay of the peak at 373 nm. Since neither dilution of the Na⁺Fl⁺ solution nor the addition of a common ion affected this interconversion, the authors eliminated the two following equilibria:

$$(Na^{\dagger}F1^{\dagger})_{2} \Longrightarrow 2(Na^{\dagger}F1^{\dagger}) \tag{10}$$

$$Na^{+}F1^{-} \longrightarrow Na^{+} + F1^{-}$$
 (11)

On the other hand, when they studied the spectra of lithium fluorenyl (Li⁺Fl⁺) in various solvents, they observed the

following

-

These res

Fl⁺,

The symbo

to be a p
The speci
Which the
solvent me
of such s

Peak at 3

a very st

dioxane.

Fl⁺,

The resultion converted

^{(A}346^{/A}37 1.15. Ot

non-diss

following:

- only a single peak at 346 nm in dioxane at 25°C;
- only one peak at 373 nm in DME;
- both peaks in THF.

These results led the authors to suggest the existence of a non-dissociative equilibrium:

$$Fl^{\dagger}$$
, Li^{\dagger} \longrightarrow Fl^{\dagger} || Li^{\dagger} (12)

The symbol Fl⁺, Li⁺ represents a "contact ion-pair", considered to be a pair of ions held together by coulombic attraction. The species Fl⁺ || Li⁺ is a "solvent-separated ion-pair" in which the cation and the anion are separated by at least one solvent molecule. In order to further test for the existence of such species, the authors added dimethyl sulfoxide (DMSO), a very strong solvating agent, to the Li⁺Fl⁺ solution in dioxane. As expected, the 346 nm peak was converted to the peak at 373 nm by the addition of DMSO:

$$F1^{\dagger}$$
, Li^{\dagger} \xrightarrow{DMSO} $F1^{\dagger}$ | Li^{\dagger} (13)

The results therefore indicated that the contact ion-pair was converted to the solvent-separated pair. A graph of log (A₃₄₆/A₃₇₃) vs. log (DMSO) gave a straight line with slope 1.15. Other studies (24,25) have also shown the existence of non-dissociative equilibria.

2.1.5.3

both equi

Hoge

fit their set of eq

Where (Ar

but are s

Anoth

by a poter

dependent

increases

Initially

solvent b

date a $s_{\mathbb{C}}$

allow a p

the syste

increases

sponding |

2.1.5.3 --Other Equilibria

Hogen-Esch and Smid (26) found that the combination of both equilibria described above

$$Ar^{-}, M^{+} \longrightarrow Ar^{-} \mid M^{+}$$

$$M^{+} + Ar^{-}$$
(14)

fit their spectroscopic and conductance data. Yet another set of equilibria was proposed by Hirota (27):

where (Ar, M, and (Ar, M, b) are both contact ion-pairs but are solvated differently.

Another model of ion-pairing was proposed by Chang,
Slates and Szwarc (28). These authors described ion-pairing
by a potential well whose shape is temperature and solvent
dependent. Presumably, the potential energy of the two ions
increases as they are pulled away from their contact position.
Initially, their mutual attraction is not attenuated by the
solvent because the gap between them is too small to accommodate a solvent molecule. But when the gap is large enough to
allow a polar solvent molecule to squeeze in, the energy of
the system decreases. Further stretching of the pair again
increases the potential energy until a limiting value (corresponding to infinite separation of the ions) is reached.

2.1.5.4--

Yet none o

We al

say at thi

sclutions

that it is

ion-pairs

solvated i

ın equilik

centration

usually pr

lon-pairir

of aromati

2.2.1--<u>The</u>

The s

anions (5;

to be:

2 22

Where Arm

carbon.

Paul

only on the

ist for t

2.1.5.4--Conclusions Regarding Ion-pairing

We already have seen more than one model of ion-pairing. Yet none of them is completely satisfactory. We can only say at this time, by restricting the scope of ion-pairing to solutions of aromatic radical anions in ethereal solvents, that it is probably correct to admit the existence of contact ion-pairs and solvent-separated ion-pairs along with the free, solvated ions. These three forms of ion-pairs are probably in equilibrium. Depending on the size of the ion, the concentration, the solvent and the temperature, one form is usually predominant over the others. We will see later that ion-pairing can drastically affect the kinetics of protonation of aromatic radical anions in ethereal solvents.

2.2--Kinetics Studies

2.2.1-- The Mechanism of Paul, Lipkin and Weissman

The stoichiometry of protonation of aromatic radical anions (Ar*) in ethereal solvents has been shown (2,29,30,31) to be:

$$2 Ar^{+} + 2 ROH \longrightarrow Ar + ArH_{2} + 2 RO^{-}$$
 (16)

where ArH is the dihydro-adduct of the parent aromatic hydrocarbon.

Paul, Lipkin and Weissman (3), basing their arguments only on the stoichiometry of the reaction, proposed a mechanism for the reaction of naphthalene radical anions (Nap*) with

either CO an alcoho

Where Napi With this decay of t

- t:

to

- t:

fa This pione

Lipkin and

2.2.2--<u>Kir</u> Krapq

Tetal-alc:

Zenes in :

an aromat

times - 1

Reach th

authors d

either CO_2 or various proton donors. For the reaction with an alcohol(ROH), the mechanism was:

$$Nap^{\bullet} + ROH \longrightarrow NapH^{\circ} + RO^{-}$$
 (17a)

$$NapH^{\bullet} + Nap^{\bullet} \longrightarrow NapH^{-} + Nap$$
 (17b)

$$NapH + ROH \longrightarrow NapH_2 + RO$$
 (17c)

where NapH₂ is the dihydro-adduct of the naphthalene molecule. With this mechanism, one would expect to find a first-order decay of the radical anion with the following assumptions:

- the electron transfer step (17b) is fast compared to the proton transfer step;
- the second proton transfer step (17c) to NapH is fast compared to the first one (17a).

This pioneering mechanism has come to be known as the Paul, Lipkin and Weissman mechanism.

2.2.2--Kinetics Studies in Ammonia

Krapcho and Bothner-By (32,33) conducted a study of the metal-alcohol reduction of benzene and some substituted benzenes in ammonia in the following way: they successively added an aromatic hydrocarbon, an alkali metal and an alcohol to liquid ammonia at -34°C. Since the reactions were slow (half-times ~ 100 sec), they could extract aliquots periodically, quench them and analyze them. From this product analysis, the authors deduced the stoichiometry:



Although

investiga
They foun

fit their mechanism

M + 9

M⁺(so

M⁺(se

M⁺ (s

Μ* (ε

Where M

species.

tetal och

Although benzene was present at the end of the reaction, the investigators considered it to be unreacted starting material. They found that a third-order rate law:

$$-\frac{d[Ar]}{dt} = k [Ar][M][ROH]$$
 (19)

fit their experimental data well. They proposed the following mechanism:

$$M + solvent \longrightarrow M^+(solv.)...e^-(solv.)$$
 (20a)

$$M^+$$
(solv.)...e (solv.) + Ar $\longrightarrow M^+$ (solv.)...Ar (solv.) (20b)

$$M^+$$
(solv.)...Ar $^-$ (solv.) + ROH \longrightarrow ArH $^+$ (solv.) + ROM(solv.) (20c)

$$M^{+}$$
 (solv.)...e (solv.) + ArH (solv.) \longrightarrow M^{+} (solv.)...
ArH (solv.)

(20d)

 M^{+} (solv.)...ArH (solv.) + ROH \longrightarrow ArH₂ + ROM(solv.)

(20e)

where M⁺(solv.), e⁻(solv.), etc. ... designate the solvated species. In addition to the first-order dependence on the metal concentration, the following observations were made:

- the reduction reaction proceeded more slowly with Na than with Li;

- 1

,

- The author

equilibri

Li

Na (s

Late

rate law :

mechanism:

In this :

In fact, reported.

Step. A

tining s

In

Rinetics

- the reaction rate was not affected by the addition of NaBr;
- The reaction rate increased upon addition of LiBr.

 The authors explained the effect of LiBr by proposing the equilibrium:

$$Li^{+}(solv.)...Br^{-}(solv.) + Na^{+}(solv.)...Ar^{-}(solv.)$$
 $Na^{+}(solv.)...Br^{-}(solv.) + Li^{+}(solv.)...Ar^{-}(solv.)$
(21)

Later, Jacobus and Eastham (34) reported a fourth-order rate law for the same system and proposed the following mechanism:

$$C_6^{H_6} + e^{-} \longrightarrow C_6^{H_6}$$
 (22a)

$$\cdot C_6^H_6^- + ROH \longrightarrow H \cdot C_6^H_6 + RO^-$$
 (22b)

$$H \cdot C_6^H + e^+ \longrightarrow H \cdot C_6^H =$$
 (22c)

$$H:C_6^{H_6} \xrightarrow{slow} C_6^{H_7}$$
 (22d)

$$C_6H_7^- + ROH \xrightarrow{fast} C_6H_8 + RO^-$$
 (22e)

In this mechanism, the alkoxide RO plays an important role. In fact, inhibition of the reaction upon addition of RO was reported. Thus step (22b) was postulated as a reversible step. Also, step (22d) was considered to be the rate determining step.

In addition, Kelly et al. (35) have reported some kinetics data for the reaction of sodium with ethanol in liquid

amonia a the react a function of Kelly the rate

- =

which corr

ethanol re law (Equationsisten:

In vi

ammonia at -33.4°C. These authors monitored the progress of the reaction by measuring the amount of hydrogen evolved as a function of time. Later, Jolly (36) showed that the data of Kelly et al. were at least qualitatively in agreement with the rate law:

$$-\frac{d[EtOH]}{dt} = \frac{k_1[EtOH][e]}{(k_2/k_3)[EtO]+[e]}$$
(23)

which corresponds to a mechanism involving a steady-state concentration of ammonium ion:

EtOH + NH₃
$$\xrightarrow{k_1}$$
 NH₄ + EtO (24a)

$$NH_4^+ + e^- \xrightarrow{k_3} NH_3 + \frac{1}{2} H_2$$
 (24b)

In view of the mechanism suggested above for the sodiumethanol reaction, Jolly (36) showed that the third-order rate law (Equation 19) obtained by Krapcho and Bothner-By was also consistent with the mechanism:

$$ROH + NH_3 \xrightarrow{k_1} NH_4^+ + RO^-$$
 (25a)

$$Ar + e^{-} \frac{fast}{Ar} Ar^{-} K = \frac{[Ar^{-}]}{[Ar][e^{-}]}$$
 (25b)

$$NH_4^+ + Ar^- \xrightarrow{k_3} NH_3 + ArH^*$$
 (25c)

$$ArH^{\bullet} + e^{-} + NH_{4}^{+} \xrightarrow{fast} ArH_{2} + NH_{3}$$
 (25d)

In fact, a

amonium i

_ <u>d!</u>

When K is

soluble, t

and Bothne

Very

statetics s

solutions

conductance

the rate 1

d [

where e arm

the follow

Eton

e am

°6 €

C₆H₇

by apply:

In fact, assuming that a steady-state concentration of the ammonium ion was achieved, this mechanism yields the rate law:

$$-\frac{d[Ar]}{dt} = \frac{k_1 k_3 K[ROH][Ar][e^-]}{k_2 [RO^-] + k_3 K[Ar][e^-]}$$
(26)

When K is small and when the metal alkoxide is only slightly soluble, this rate law reduces to that obtained by Krapcho and Bothner-By (Equation 19).

Very recently, Kahn and Dewald (37) have undertaken a kinetics study of the reduction of benzene by sodium-ammonia solutions at -45°C, using ethanol as the proton source. Their conductance data showed that the reduction reactions followed the rate law:

$$-\frac{d[e_{am}]}{dt} = k[EtOH][e_{am}]$$
 (27)

where e_{am}^- is the solvated electron in ammonia. They proposed the following mechanism:

$$EtOH + NH_3 \xrightarrow{k_1} NH_4^+ + EtO^-$$
 (28a)

$$e_{am}^{-} + NH_4^{+} \xrightarrow{k_3} NH_4$$
 (28b)

$$C_{6}^{H_{6}} + NH_{4} \xrightarrow{k_{4}} C_{6}^{H_{7}} + NH_{3}$$
 (28c)

$$C_6^{H_7} + NH_4 \xrightarrow{k_5} C_6^{H_8} + NH_3$$
 (28d)

By applying the steady-state approximation to the ammonium

radical c

ď

When the this rate

k

2.2.3--<u>Pu</u> Besi

and by red

can also

hydrocarb

tion. In produced

accelerat

dissolved

ethanol

ctserved

then deci

tion spe

to those

reduced .

te ident

diced th.

radical concentration, the rate law becomes:

$$-\frac{d[e_{am}]}{dt} = \frac{k_3 k_1 [EtOH] [e_{am}] [NH_3]}{k_2 [EtO^-]}$$
 (29)

When the reaction mixture is saturated with sodium ethoxide, this rate law yields Equation 27 in which:

$$k = \frac{k_3 k_1 [NH_3]}{k_2 [EtO]}$$
 (30)

2.2.3--Pulse-radiolysis Studies

Besides their production by electrochemical reduction and by reduction with alkali metals, aromatic radical anions can also be generated via reduction of the parent aromatic hydrocarbon by solvated electrons produced by ionizing radia-In the pulse-radiolysis technique, ionization is produced by a burst of high-energy electrons from a linear accelerator. In some early studies, aromatic hydrocarbons were dissolved in pure solvents such as cyclohexane (38) and ethanol (39), bombarded with high energy electrons and then observed spectroscopically. Absorbing species were formed which then decayed completely within a few microseconds. The absorption spectra of these species often corresponded very closely to those obtained when the same aromatic hydrocarbons were reduced with alkali metals. Thus these transient species could be identified as the well known aromatic radical anions produced this time by the reaction:



Rate cons

(39,40).

In pure a

to follow

The autho

The rate

anthracer

range fro

8.1 x 10 anion, ti

rates.

In picture

ions by

such as

is form

hand, or

$$Ar + e^{-}(solv.) \longrightarrow Ar^{-}$$
 (31)

(note however that radical cations have similar spectra).

Rate constants for this formation reaction were found to be about 10⁹M⁻¹sec⁻¹ depending on the aromatic hydrocarbon used (39,40). In some solvents, triplet states of the aromatic molecules and aromatic radical cations were formed (39,41).

In pure alcohols, the aromatic radical anions were reported to follow a fast first-order decay:

$$-\frac{d[Ar^{\dagger}]}{dt} = k'[Ar^{\dagger}]$$
 (32)

The authors (39,40) suggested a proton transfer from the alcohols as follows:

$$Ar^{-} + ROH \longrightarrow ArH^{\circ} + RO^{-}$$
 (33)

The rate constants for this reaction were determined for anthracene, biphenyl and terphenyl in four alcohols. They range from $2 \times 10^2 \text{M}^{-1} \text{sec}^{-1}$ for terphenyl in ethanol to $8.1 \times 10^4 \text{M}^{-1} \text{sec}^{-1}$ for anthracene in methanol. For a given anion, the more acidic alcohols gave the higher protonation rates.

In a recent article (40), Dorfman presented an overall picture of the mechanism of the formation of aromatic radical ions by pulse-radiolysis techniques. In polar protic solvents, such as the aliphatic alcohols, only the radical anion (Ar*) is formed. In certain chlorinated hydrocarbons, on the other hand, only the radical cation (Ar*) is produced. In non-polar

aprotic

and the

In

the acti

The elec-

Then a se

The solve

ion (RCH)

म्रू (Eda)

Pul.

esting i

transfer in ethy:

bipheny [

Mien the

Solvent,

rerains

aprotic solvents such as cyclohexane, both the radical anion and the radical cation are formed.

In the alphatic alcohols, the proposed mechanism for the action of ionizing radiation was:

$$ROH \longrightarrow ROH^+ + e^-$$
 (34)

The electrons produced in this step are rapidly solvated.

Then a sequence of reactions can occur as follows:

$$e^{-}(solv.) + Ar \longrightarrow Ar^{-}$$
 (31)

$$Ar^{-} + ROH \longrightarrow ArH^{\cdot} + RO^{-}$$
 (33)

$$ROH^{+} + ROH \longrightarrow ROH_{2}^{+} + RO^{-}$$
 (35)

$$Ar^{\bullet} + ROH_2^{+} \longrightarrow ArH^{\circ} + ROH$$
 (36)

The solvent counter ion ROH^+ rapidly forms the alkyloxonium ion (ROH_2^+) (Equation 35) which then reacts very rapidly with Ar^- (Equation 36).

Pulse radiolysis in mixed solvents (40,42) gave interesting information about solvent effects on the protontransfer rates. In fact, irradiation of biphenyl solutions in ethylene diamine and in triethylamine gave a lifetime of biphenylide which was about 100 times greater than in ethanol. When the investigators added ethanol to ethylenediamine as solvent, they found that the lifetime of the biphenylide ion remains virtually unchanged up to a concentration of about



65 mol %

reactive

the decr

weakenin

alcohol

Irradiat

ixtures

increase:

of the pr

mution h

concomers,

by hydrog

2.2.4--<u>K</u>:

Usin

Themoto

radical a

illethy):

10) that

addition.

ipon the

et the e

te firs

ipon the

Posed ti

65 mol % ethanol. An extensive hydrogen bonding of the reactive alcohol proton to the amine was suggested to explain the decrease in the rate constant. On the other hand, weakening of the hydrogen bonded solvent structure of the alcohol would be expected for non-polar hydrocarbon solvents. Irradiation of a solution of biphenyl in ethanol-cyclohexane mixtures showed that the first-order decay constant actually increased over the value in pure ethanol. This enhancement of the protonation rate was interpreted as due to the disruption by the cyclohexane of an equilibrium system of monomers, dimers and polymers of ethanol units held together by hydrogen bonds.

2.2.4--Kinetics Study Using ESR and Polarography

Using a combination of ESR and polarographic techniques, Umemoto (43) studied the protonation by water of anthracene radical anions which were electrochemically generated in N,N'-dimethylformamide (DMF). It has been mentioned earlier (9, 10) that d.c. polarograms showed two reversible one-electron additions to the anthracene molecule in dry DMF as solvent. Upon the addition of water, the first wave increased in height at the expense of the second. Also, the reversible peak of the first wave in the a.c. polarogram decreased remarkably upon the addition of a small amount of water. Umemoto proposed the following mechanism to explain these results:

where And decay in step (37) tration

of the r

Since th

A first-

first-or

concentr interpre

the pres

Ume followed

2.2.5--

R€.

tonatic: mixture

$$An^{-} + H_2O \xrightarrow{k'} AnH^{-} + OH^{-}$$
 (37a)

$$AnH^{\bullet} + An^{\bullet} \longrightarrow AnH^{-} + An$$
 (37b)

$$AnH^{-} + H_{2}^{O} \longrightarrow AnH_{2} + OH^{-}$$
 (37c)

where AnH₂ is the dihydroproduct of anthracene. A first-order decay in An^{*} was derived from this mechanism by assuming that step (37a) is irreversible and that the steady-state concentration for the species AnH^{*} was achieved. This gives:

$$-\frac{d[An^{\dagger}]}{dt} = 2k'[An^{\dagger}][H_2O]$$
 (38)

Since the protonation reaction was relatively slow, the decay of the radical anion in the presence of water could be studied by observing changes in the ESR signal intensity with time. A first-order curve was observed up to 6% H₂O. However, the first-order rate constant did not increase linearly with water concentration as predicted by Equation 38. This result was interpreted as due to change in the solvent composition in the presence of high water concentrations.

Umemoto also found that the benzophenone radical anion followed a mixed first- and second-order decay.

2.2.5--Combined Polarography-ESR-UV Absorption Spectroscopy Studies

Recently, Hayano and Fujihira (44,45) studied the protonation of numerous aromatic radical anions in DMF-water mixtures. They used three methods, polarography, ESR, and

wabsorp

Ar conce
currents
intensity
sion curr
of the Ed
to be du
spin exc
molecule
ile abso

Which is Again, a fast, th

Hayano a

Was der Or.

Jy- wa-

Preted

UV absorption spectroscopy, to simultaneously measure the Ar concentration. A linear relationship between the diffusion currents and the absorbance was found. But the ESR signal intensity showed no linear relationship with either the diffusion current or the absorbance. This non-linear dependence of the ESR signal intensity on the Ar concentration was found to be due to the broadening caused by the rapid intermolecular spin exchange, even when the concentration of the parent molecule, Ar, was constant. The change with time of the visible absorption band of Ar followed a first-order rate law. Hayano and Fujihira proposed the following mechanism:

$$Ar^{-} + H_2O \xrightarrow{k} ArH^{\cdot} + OH^{-}$$
 (39a)

$$ArH^{\bullet} + Ar^{\bullet} \longrightarrow ArH^{-} + Ar$$
 (39b)

$$ArH^{-} + H_{2}O \xrightarrow{k'} ArH_{2} + OH^{-}$$
 (39c)

which is identical to the Umemoto mechanism (Equations 37a,b,c). Again, assuming that step (39a) is slow, but step (39b) is fast, the rate equation:

$$-\frac{d[Ar^{\top}]}{dt} = 2k [H_2O][Ar^{\top}]$$
 (40)

was derived, which is identical to Equation 38.

Once again, the protonation rate by water was found to be greatly accelerated by increasing the water concentrations in DMF-water mixtures. The reason for this behavior was interpreted (45) as follows: the negative charge is more localized

changin be inte the cha chargetransfe

on a ce

inal ar

complex

2.2.6--

Ar

in sect and Hay to gene

thracen

protona

pseudo

Di

Which v

Thanalyze

possibl

on a certain atom in the activated complex than in the original aromatic radical anions (Ar^{*}). Therefore, the activated complex is more stabilized than is the original Ar^{*} by changing the solvent from aprotic to protic. The reaction can be interpreted as a transfer process between the no-bond and the charge-transfer structures. The activated complex is a charge-transfer complex in which the no-bond and charge-transfer structures contribute almost equally to the resonance.

2.2.6--Kinetics Studies Using Polarography and Stopped-flow

Another way of investigating the same problem as described in sections 2.2.4 and 2.2.5 was undertaken by Fujihira, Suzuki and Hayano (46). These authors used electrochemical reduction to generate the radical anions of anthracene and 1,2-benzan-thracene. They used the stopped-flow technique to study the protonation with $\rm H_2O$ in DMF.

Direct measurements by the stopped-flow method gave a pseudo first-order decay:

$$-\frac{d[Ar^{*}]}{dt} = -2k[H_2O][Ar^{*}]$$
 (40)

$$= -k_{app} [Ar^{T}]$$
 (41)

which was in agreement with mechanism (39).

The results obtained from the polarographic method were analyzed by using rigorous mathematical treatments for the two possible mechanisms (3) and (39). The values of $k_{\rm app}$ obtained



by the application of mechanism (39) to the polarographic data agreed well with those obtained by the stopped-flow technique.

2.2.7--Stopped-flow Studies

The stopped-flow technique is suitable for the study of fast protonation reactions of aromatic radical anions with alcohols in ethereal solvents. In fact, this technique has been adopted recently by many investigators including Minnich and Dye (47,48), Bank and Bockrath (49,50) and Szwarc and coworkers (51,52).

2.2.7.1--The Work of Minnich

Minnich studied the reactions of the radical anions of anthracene (An) and terphenyl (Ter) with alcohols and with water in two ethereal solvents, THF and DME (47,48). The radical anions were produced by reduction of the parent molecules with Na and K. The reaction rates were followed spectrophotometrically by using a scanning stopped-flow apparatus.

In THF, the reactions of K⁺An⁻ with EtOH, MeOH, t-BuOH, i-PrOH and H₂O were reported for the first time (47) to have a second-order behavior in the absorbance. The order in ROH was less than unity. Only limited ranges of the alcohol concentrations were studied. Also the concentration of anthracene remained nearly the same in many experiments. Variation of the alkoxide concentration (RO⁻) had no effect on the reaction rates.

Similar results were obtained for the reactions in DME, but the pseudo second-order rate constants were an order of magnitude lower ($k_{THF} \sim 1 \times 10^4 M^{-1} sec^{-1}$; $k_{DME} \sim 1 \times 10^3 M^{-1} sec^{-1}$).

The reactions of Na⁺An⁺ with EtOH in THF were similar to those of K⁺An⁺ in the same solvent. The reaction with H₂O of Na⁺An⁺ in THF was studied in two separate experiments. In one case, pseudo second-order decay was observed, but in the other case, a mixed pseudo first- and second-order was seen with a large first-order contribution. Due to this inconsistency, no quantitative results were obtained for this reaction.

Striking differences were reported for the reaction of Na⁺An⁻ with EtOH or with H₂O in DME. The decay of Na⁺An⁻ in DME was much slower than in THF and it followed a first-order rate law in the absorbance. Also, the reaction of K⁺Ter⁻ with EtOH in THF was found to be fast and first-order in each reactant.

These results were consistent with the following proposed mechanism:

$$An^{-}, M^{+} + An^{-}, M^{+} \xrightarrow{k_{+}^{+}} (An^{-}, M^{+})_{2}$$
 (42a)

$$(An^{-}, M^{+})_{2} + ROH \xrightarrow{k_{1}^{+}} M^{+}AnH^{-} + An + M^{+}, RO^{-}$$
 (42b)

$$M^{+}AnH^{-} + ROH \xrightarrow{k_{2}} AnH_{2} + M^{+}, RO^{-}$$
 (42c)

An,
$$M^{+} + ROH \xrightarrow{k_3} M^{+}, RO^{-} + AnH$$
 (42d)

An,
$$M^+ + AnH$$
 $\frac{k_4}{fast}$ $M^+AnH^- + An$ (42e)

If a steady-state concentration for the species (An, M, M), was made, the general rate law could be derived:

$$-\frac{d[An^{-}, M^{+}]}{dt} = \left(\frac{2k_{+}^{+}}{1 + \frac{k_{-}^{+}}{k_{1}^{+}[ROH]}}\right) [An^{-}, M^{+}]^{2}$$

$$+ k_{3}[An^{-}, M^{+}][ROH]$$
(43)

In cases where contact ion-pair formation is favored (at least at low values of [ROH]), the second-order process predominates (Equations 42a,b,c). When such ion-pairing is not favored, the first-order process is seen (Equations 42d,e,c).

2.2.7.2-- The Studies of Bank and Bockrath

For their first kinetics study with a stopped-flow device, Bank and Bockrath (49) chose the reaction of sodium naphthalenide (Na⁺Nap⁺) with H₂O in THF. The naphthalene radical anion was produced by the normal method of reduction of naphthalene (Nap) with metallic sodium. The authors found that the decay of Na⁺Nap⁺ followed a pseudo first-order rate law in agreement with the Paul, Lipkin and Weissman mechanism (Equations 17a,b,c):

$$Nap^{-} + H_2O \xrightarrow{k_1} NapH^{\cdot} + OH^{-}$$
 (44a)

$$NapH^{\bullet} + Nap^{\bullet} \xrightarrow{k_2} NapH^{-} + Nap$$
 (44b)

$$NapH^{-} + H_{2}O \xrightarrow{k_{3}} NapH_{2} + OH^{-}$$
 (44c)

where NapH₂ is the dihydroproduct of naphthalene. Again, assuming a steady-state concentration of the species (NapH°), the pseudo first-order rate law was derived:

$$-\frac{d[Nap^{*}]}{dt} = 2k_{1}[H_{2}O][Nap^{*}] = 2k_{1}[Nap^{*}]$$
 (45)

where

$$k_1' = k_1[H_2O]$$

The value of k_1 at 20°C was found as:

$$k_1 = 1.01 \times 10^4 \text{M}^{-1} \text{sec}^{-1}$$
.

Very recently, the same authors studied the kinetics of the reaction of sodium anthracenide (Na⁺An⁺) with H₂O in THF, DME and mixtures of these solvents (50). For this study, instead of preparing the An⁺ in the usual way, they used naphthalenide (Nap⁺) (produced from reaction of naphthalene with sodium metal) to reduce An to An⁺:

$$Nap^{T} + An \longrightarrow An^{T} + Nap$$
 (46)

They made the three following assumptions to validate this method:

- a) the electron transfer to An is kinetically faster than the protonation of Nap*;
- b) the concentration of Na Nap in equilibrium with Na An is kinetically insignificant;
- c) the equilibrium concentration of the anthracene dianion is also kinetically insignificant.

Once more, the reaction of $Na^{\dagger}An^{\dagger}$ with H_2^{0} in THF was reported to be similar to the reaction of $Na^{\dagger}Nap^{\dagger}$ with H_2^{0} in the same solvent. Thus, the Paul, Lipkin and Weissman mechanism was apparently once more confirmed. However, $Na^{\dagger}An^{\dagger}$ was reported to be considerably less reactive than $Na^{\dagger}Nap^{\dagger}$ ($k(Nap)/k(An) \approx 182$). When sodium tetraphenylboron was added to the stock solution of $Na^{\dagger}An^{\dagger}$ in DME, the observed rate constant increased more than 20-fold. Further addition however did not have much effect on the reaction rate. The authors presumed that the sodium ion solvates a water molecule significantly better than the ether. The water molecule so solvated is more "acidic" than either free or solvent-solvated water. Note however that these experimental results are in disagreement with the results of Szwarc when DME was used as solvent and also with our results in THF (see later).

2.2.7.3--The Studies of Szwarc and Co-workers

The kinetics study of Levin, Sutphen and Szwarc (51) involved the reaction of sodium perylenide (Na⁺Pe⁺) by alcohols and by water in THF at 25°C. The mode of preparation of the perylene radical anion was the standard reduction of perylene (Pe) with Na. The protonation reaction was shown to be second-order in Na⁺Pe⁺, first-order in ROH and inverse first-order in Pe. The ion-pair of the perylenide dianion served as the base according to the "dianion mechanism":

$$2Pe^{-}$$
, $Na^{+} \xrightarrow{K_{1}} Pe^{-}$, $2Na^{+} + Pe$ (47a)

$$Pe^{-}$$
, $2Na^{+}$ + ROH \xrightarrow{k} Na^{+} PeH $^{-}$ + Na^{+} RO $^{-}$ (47b)

$$Na^{+}PeH^{-} + ROH \xrightarrow{fast} PeH_{2} + Na^{+}RO^{-}$$
 (47c)

The rate expression was:

$$-\frac{d[Pe^{-}, Na^{+}]}{dt} = \frac{2kK_{1}[ROH][Pe^{-}, Na^{+}]^{2}}{[Pe]}$$
(48)

The relative values of k were found to increase with the acidity of the alcohol used.

Very recently, Rainis, Tung and Szwarc (52) investigated the protonation of sodium anthracenide (Na⁺An⁺) with alcohols and with water in DME, a stronger solvating agent than THF.

The following interesting results were reported:

First, the protonation by MeOH, EtOH, i-PrOH and H₂O was first-order in Na⁺An⁻ in agreement with the results of Minnich and Dye (47,48), but mixed first- and second-order in ROH.

The authors proposed that the dimeric species (ROH)₂ formed by:

$$2ROH \xrightarrow{K_d} (ROH)_2$$
 (49)

participates in the protonation process. The reactions:

$$An^{+}$$
, Na^{+} + ROH \longrightarrow AnH $^{\circ}$ + RO $^{-}$, Na^{+} (50a)

or

$$An^{\dagger}$$
, Na^{\dagger} + (ROH)₂ \longrightarrow AnH° + RO⁻, Na^{\dagger} + ROH (50b)

are rate determining.

Second, the protonation with t-BuOH was reported to we a second-order dependence in (Na⁺An⁺). A new mechanism proposed to explain this result:

$$An^{-}$$
, Na^{+}) $\stackrel{k_{f}}{\rightleftharpoons}$ $(An^{-}$, Na^{+}) $2 \stackrel{k'_{f}}{\rightleftharpoons}$ $(An^{=}$, $2Na^{+}$; An) (51a)

$$An^{-}$$
, $2Na^{+}$; $An) + ROH \xrightarrow{k_{p}^{+}} AnH^{-}$, $Na^{+} + An + RO^{-}$, Na^{+} (51b)

The species (An⁼, 2Na⁺; An) is called the "solvent caged" complex and is presumed to be the most probable protonated base. This species can also generate the "diffused out of cage" complex (An⁼, 2Na⁺) which is the ion-paired dianion of anthracene:

$$2(An^{-}, Na^{+}) \xrightarrow{K} (An^{-}, Na^{+})_{2} \xrightarrow{K'} (An^{+}, 2Na^{+}; An)$$

$$\xrightarrow{K''} An^{-}, 2Na^{+} + An \qquad (52)$$

Thus the pseudo second-order rate constant is only slightly affected by the variation of [An] although it increases with [ROH]. In their interpretation of the results, Rainis, Tung and Szwarc made use of a preprint of the work reported in this thesis (53).

In summary, the protonation of aromatic radical anions by alcohols has been investigated in diverse media, with various techniques. On the one hand, the Paul, Lipkin and Weissman mechanism, which leads to first-order behavior, seems to have been verified in some systems by many investigators.

On the other hand, recent stopped-flow studies reveal a second-order behavior in the absorbance. This proves the existence of intermediate species which are protonated.

However, the detailed nature of these intermediate species is uncertain and different mechanisms propose different intermediates. One of the major contributions of the present work is that it permits us to rule out certain mechanisms and to suggest the nature of the intermediate species.

III. EXPERIMENTAL

3.1--Vacuum Techniques

Since solutions of aromatic radical anions are very unstable in the presence of air, high vacuum techniques are required to handle every transfer of liquid from one glass container to another. A greaseless vacuum system was built for this purpose. The vacuum manifold was first pumped to about 3×10^{-3} torr with a mechanical pump. A Veeco air-cooled diffusion pump which uses Dow Corning 704 diffusion pump oil then brought the system to pressures of 2×10^{-6} torr. The vacuum line was separated from the two pumps by a liquid nitrogen trap. The manifold was also connected to a reservoir of helium gas through a purification system to be described later.

3.2--Cleaning Techniques

In order to eliminate insofar as possible every trace of impurities which could react with anion solutions and eventually lead to erronous results, careful cleaning of all glassware was necessary prior to solution preparation.

The general cleaning procedure for every piece of glassware was as follows: The item was first soaked in HF cleaner whose composition (in volume percent) was: 60% distilled water

33% HNO3, Fisher reagent grade

5% HF, 48%, Baker reagent grade

2% acid soluble detergent.

he glassware was then rinsed many times with distilled water before being soaked in aqua regia for at least half a day. Finally, about ten rinses with distilled water followed by five rinses with conductance water terminated the cleaning procedure. The item was then flamed-out and pumped to pressures of 5×10^{-6} torr to get rid of traces of water before being used in the preparation of various solutions.

The stopped-flow system which constitutes the main tool for this study was also cleaned as described above, except that HF cleaner was not used in this case since it might attack the inner parts of the mixing cell. After cleaning, the system was also pumped to at least 1×10^{-5} torr for several days before a kinetics run.

3.3--Purification Techniques

3.3.1--Tetrahydrofuran

Tetrahydrofuran (THF), the only solvent used in this study, was obtained from Burdick and Jackson ("Distilled in Glass" type). The purification procedure was slightly modified from that of Minnich (48). About 3 liters of THF were poured into a large glass vessel containing approximately 10 grams of purified grade CaH₂ (from Fisher Scientific Company).

A Teflon-coated magnet stirred the THF-CaH₂ mixture for several days until bubbles were no longer formed. The THF solvent was then vacuum-distilled into a spherical glass vessel which contained about 6 grams of benzophenone (from Eastman-Kodak Company) and an excess of a 1 to 3 sodium-potassium alloy. A purple color appeared almost immediately because of the formation of benzophenone ketyl. Because of its reactivity with water, this served both as a drying agent and as an indicator of dryness. This purple solution retained its color for months at room temperature. The THF actually used in the kinetics experiments was vacuum distilled from the purple solution thus prepared.

3.3.2--Alcohols

Spectral grade absolute ethanol (from Commercial Solvent Co.) was degassed on the vacuum line by freezing with liquid nitrogen, pumping and thawing many times until the pressure of the alcohol in the frozen state stabilized to about 2×10^{-5} torr. In the second series of experiments, ethanol was first distilled into a glass vessel containing a thin mirror of sodium and pumped out from time to time to avoid possible excessive pressure build-up due to the formation of hydrogen gas. The treatment of ethanol with sodium was aimed at the elimination of possible traces of peroxide in the alcohol. Then the ethanol was distilled into another glass ressel where the freeze-pump-thaw technique described earlier as used.

3.3.3--Alkali metals

Potassium metal as commercially available is neither pure nor convenient to use. Therefore, it was stored in short lengths of thin glass tubing such that the desired amount of metal could be easily provided.

For this purpose, lumps of potassium metal were cut into small pieces and quickly put into a tall glass vessel. Many long, thin glass tubes of 3 mm I.D. with their top ends sealed were also introduced into the same vessel which was then pumped to a pressure of about 3 x 10⁻⁵ torr. Then the vessel was moderately heated until the metal melted. At this point, helium gas was introduced into the vessel to force the molten metal up into the glass tubes. Potassium thus prepared, after solidifying, was convenient and ready for use.

3.3.4--Anthracene and Crown

Zone-refined anthracene from James Hinton Co., Valparaiso, Florida, and dicyclohexyl-18-crown-6 from E. I. du Pont de Nemours Co., were used without further purification.

3.3.5--Helium

Grade A helium from Liquid Carbonic Company was treated as follows before being admitted into the reaction vessels.

It was successively passed over hot copper shavings, hot copper oxide, through Ascarite and finally through a liquid nitrogen trap.

3.4--Preparation

3.4.1--Pre-rinsing Techniques

Before being used in the preparation of the solutions, every glass vessel was pre-rinsed with a solution of potassium anthracenide in THF especially prepared for this purpose. The glass bottle A (Figure 1) to be pre-rinsed was attached to the closed glass vessel B which contained the rinsing solution. The attachment was made by means of a T-joint which could be connected to the vacuum line. After a pressure of 1 x 10⁻⁵ torr or less had been reached, the whole system was disconnected from the vacuum line. Then, the rinsing solution was poured back and forth two or three times. In the final step, the rinsing solution was poured back into vessel B, and the THF solvent was distilled several times from B into A to eliminate traces of solute remaining on the walls of vessel A.

This technique, while time-consuming, has proven to be very helpful in the preparation of stable solutions for the kinetics experiments.

3.4.2--Anthracene and Crown Solutions

Weighed amounts of anthracene (or crown) were put into a glass tube which had a break-seal on one end and a 5 mm Fisher-Porter joint on the other. The glass tube containing An (or crown) was then attached to the vacuum line through a liquid nitrogen trap and pumped to a pressure of 5×10^{-6} torr before

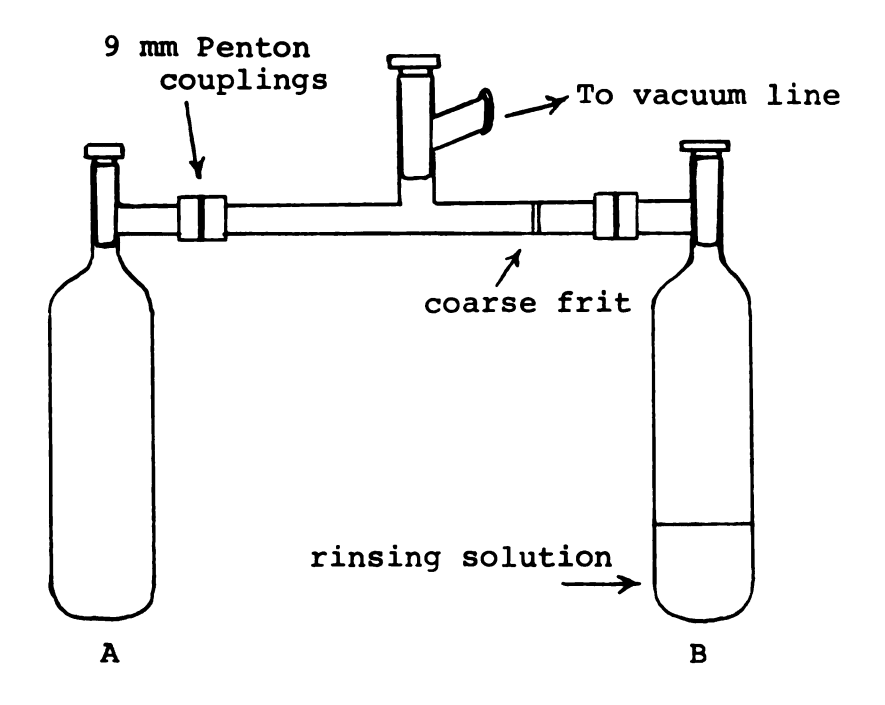


Figure 1. Special set-up for pre-rinsing technique.

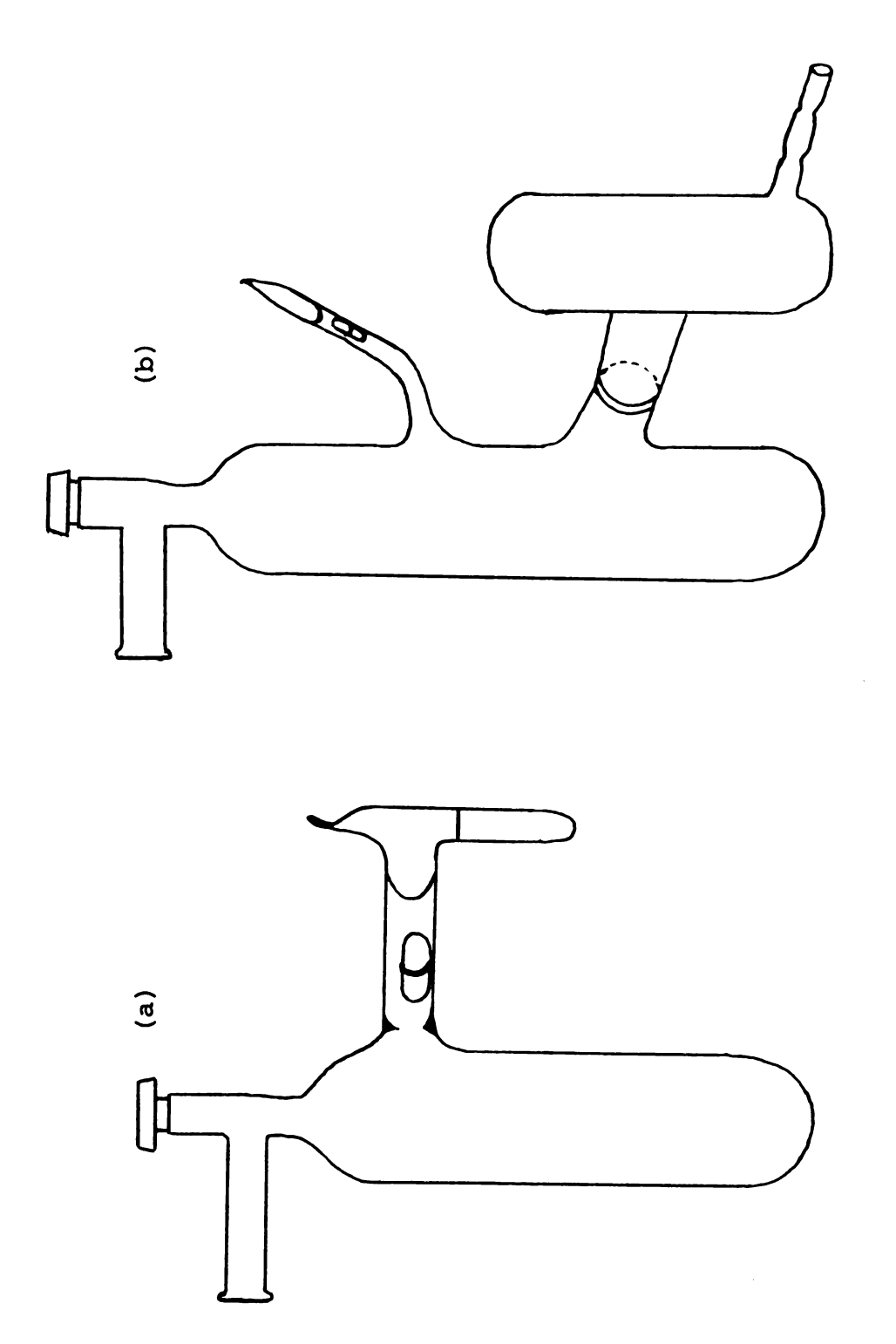
being sealed off. The amount of An (or crown) used was determined by noting the weights of the break-seal with and without An (or crown). The break-seal prepared in this way was then sealed to a side-arm of the reaction vessel (Figure 2a). This vessel was then weighed and pumped to a pressure of about 3 x 10⁻⁶ torr. The solvent (THF) was then distilled into the reaction vessel and covered with helium gas at a pressure of about 1 atmosphere. The whole apparatus was weighed again to determine the exact amount of THF used. Finally, a Teflon-enclosed magnet in the side-arm of the vessel was used to break the break-seal and An (or crown) was dissolved in the THF solvent.

3.4.3--Alcohol Solutions

Pure alcohol was distilled from its storage vessel into a glass tube with a break-seal on one end. It was then frozen with liquid nitrogen and pumped on before the glass tubing was sealed off. Weights of the break-seal tubing with and without alcohol in it gave the exact amount of alcohol used. The break-seal was then connected to the side-arm of a reaction vessel (Figure 2a) and the process of distilling THF solvent and admitting helium gas into the vessel was exactly the same as described earlier in section 3.4.2.

3.4.4.--Anion Solutions

Solutions of potassium anthracenide were prepared in special glass vessels as shown in Figure 2b. A break-seal



Vessels used in the preparation of: (a) An, crown or ROH solutions (b) K+An solutions. Figure 2.

containing a known amount of anthracene was sealed onto a side-arm on one side of the glass vessel. A second side-arm on the other side of the vessel was constricted at four or five places. A small length of tubing which contained potassium metal (as described in section 3.3.3) was introduced into the side-arm and it was sealed off at the end. vessel was then pumped to a pressure of 5×10^{-6} torr or less before the potassium metal was gently heated. The glass constrictions were then sealed off one by one after the metal had been distilled through each of them. In this way, the metal underwent four or five independent distillation steps, leaving oxide behind, before it was distilled into the special vessel in the form of a shiny mirror of pure potassium metal. After introduction of the metal, THF was distilled into the non-metal side of the vessel, and helium gas was admitted. After the break-seal had been broken by a Teflon enclosed magnet, the anthracene was dissolved in the THF. About half of the anthracene solution was poured into the metal part of the vessel through a coarse frit. A blue color appeared as soon as the anthracene solution contacted the potassium metal. This color grew deeper with time. When it was judged that it would give an absorbance between one and two absorbance units in the flow system, the blue solution was poured back into the non-metal part where it was mixed with the remaining anthracene solution. This method of preparation of anthracenide solutions prevented the formation of the anthracene

dianion since an excess of anthracene was always present in the blue solution. Differences in the weights of the vessel with and without THF gave the amount of solvent present. The vessel was then attached to the stopped-flow system, and the long-awaited kinetics experiment could begin.

3.5-- The Stopped-flow Experiment

3.5.1--General

Conventional methods of mixing and analysis are too slow to be used in the study of fast reactions whose half-times range from a few milliseconds to a few seconds. Stopped-flow techniques possess two main advantages over conventional techniques. These are fast mixing and fast analysis, thus allowing one to study very fast reactions.

3.5.2-- The Stopped-flow Apparatus

The stopped-flow system can be roughly divided into three parts (Figure 3) which we will refer to as the left, the right and the central parts. The left and right parts are the same. Each one is composed of a burette and a mixing vessel which were used to prepare solutions of various reactants. These were introduced into the system via 9 mm Fisher-Porter Solv-Seal joints located above each burette. The burettes were standard 50 ml Pyrex burettes calibrated to 0.1 ml. Volume readings were estimated to 0.01 ml. Mixing was performed by stirring the solution with a Teflon-encased magnet which had

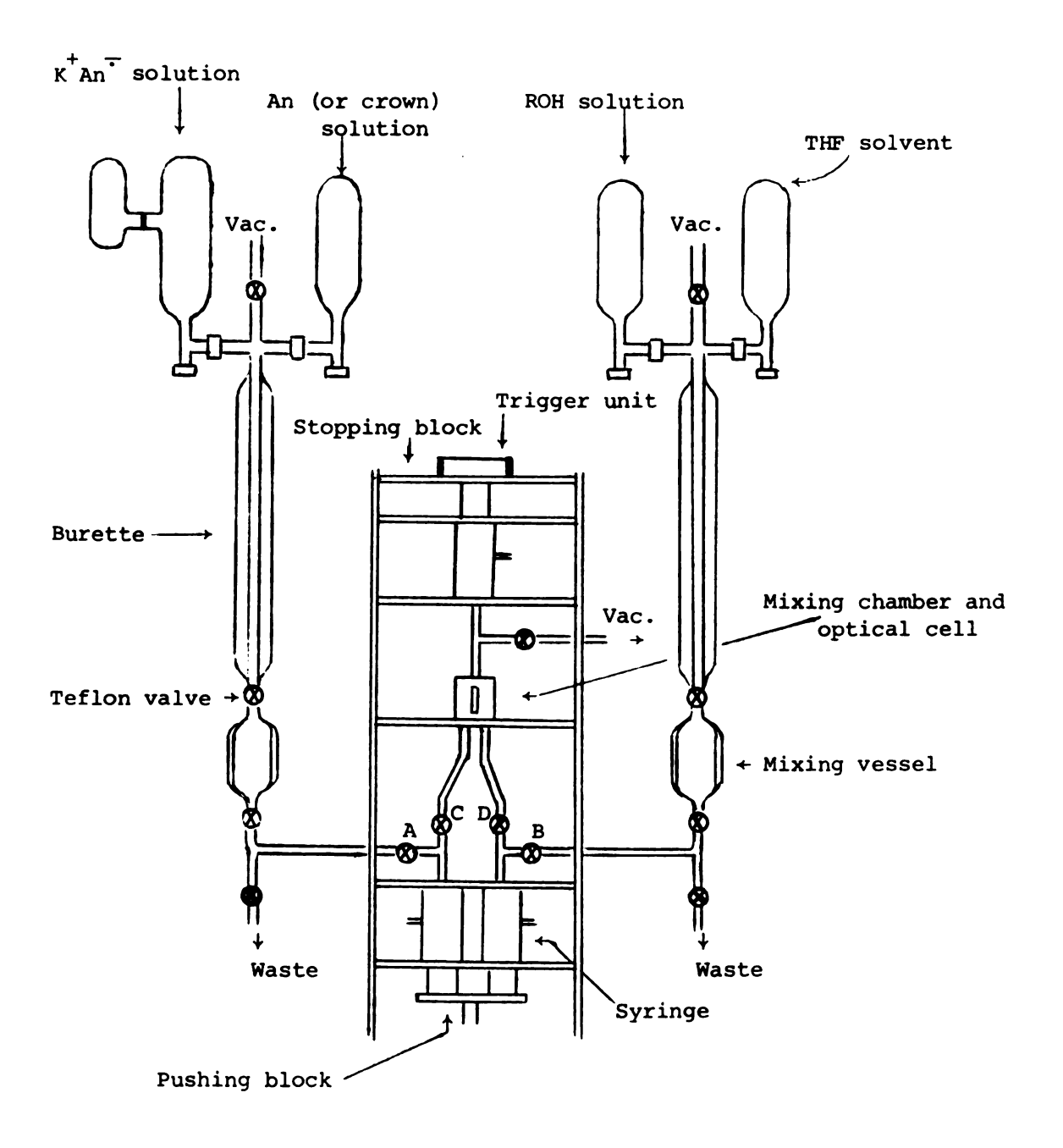


Figure 3. Schematic diagram of the stopped-flow apparatus.

been sealed inside the mixing vessel. To empty the bottom tubes, the solution was often warmed to boiling with a heat gun or with just the heat from one's hand.

The central part of the stopped-flow apparatus is more complex and thus deserves more attention in its description. The main components of this part are: a pair of pushing syringes with Teflon plungers, appropriate valves, a mixing cell and a stopping syringe. All of these components were tightly held together by a set of aluminum plates with threaded 3/8 inch brass rods, and the whole system was bolted to a rigid table made of two inch angle iron of 1/4 inch thickness.

Since THF attacks Viton-A "O-rings" and dissolves most stopcock greases, a special design was needed for a greaseless and air-tight syringe for the stopped-flow system. The final model of such a syringe (Figure 4) was evolved after many tests by Drs. V. A. Nicely, M. G. DeBacker and E. R. Minnich. These syringes were made of precision bore tubing (Trubore 8700-60, Ace Glass Inc.) with a side-arm sealed at the midpoint of the syringe and a 5 mm Fisher-Porter Solv-Seal joint at one end. The Teflon plungers have two sets of double Teflon ridges so that gases which are trapped between the pairs of ridges can be pumped out constantly through the side-arms.

Needle-valve type stopcocks used in the stopped-flow system were of two kinds: Fisher-Porter Lab-Crest 4 mm Quick Opening Valves and Delmar-Urry valves. The first ones had

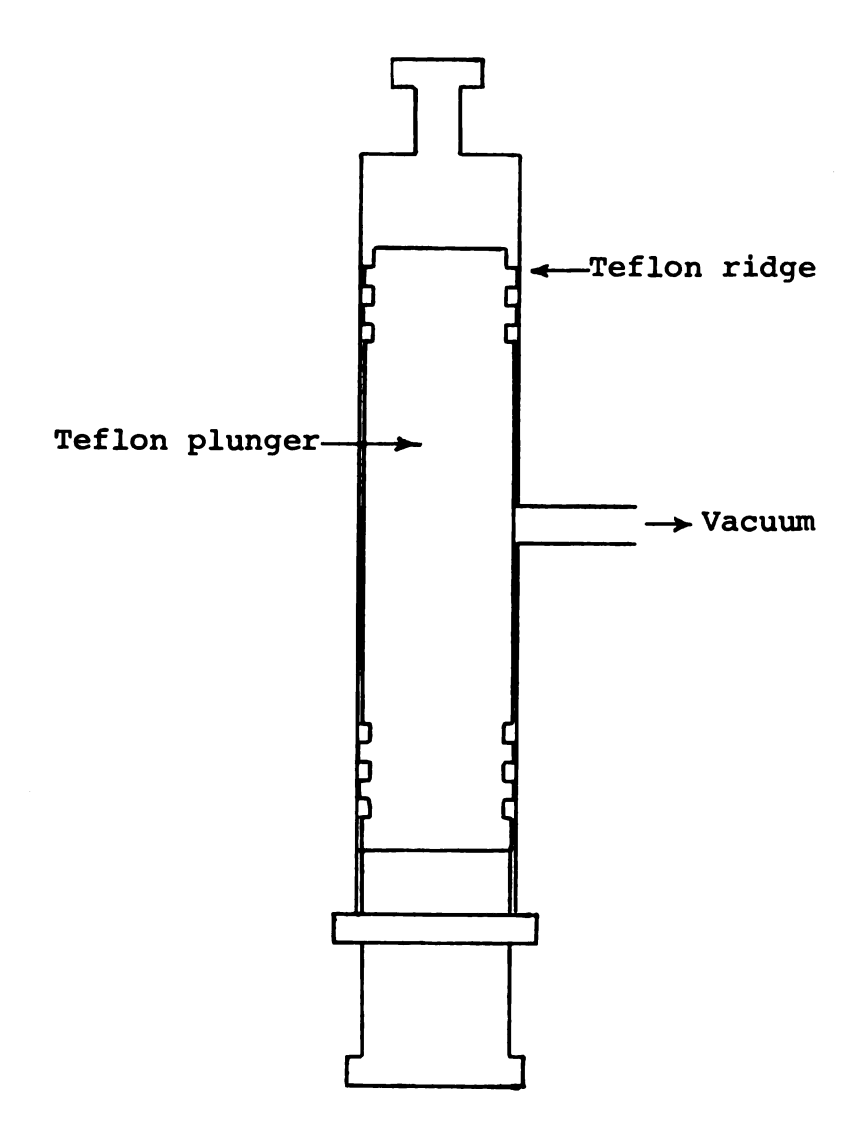


Figure 4. Syringe used in the stopped-flow system.

Teflon tape wrapped around the threaded parts. The second ones had two of their four "O-rings" replaced by Teflon.

To accomplish this, the entire Teflon valve stem was constructed in the Chemistry Machine Shop.

The design and construction of the four-jet quartz mixing cell (Figures 5a,b) used in this stopped-flow system is described by Hansen (54). The cell has two flat faces and is approximately 1.0 mm I.D.

3.5.3--Calibration of the Stopped-flow System

The stopped-flow apparatus was calibrated in the following way:

A freshly prepared stock solution of KMnO $_4$ in H $_2$ O at a concentration C $_0$ was successively diluted to make three more solutions at concentrations 0.75 C $_0$, 0.50 C $_0$ and 0.25 C $_0$. The absorbances of the 526 nm peak of these various KMnO $_4$ solutions were then measured on a Cary 14 spectrophotometer with (1.00 \pm 0.01) mm SCC cells. On the other hand, a digital voltmeter (Heath Universal Digital Instrument, model EU-805) was used to read the corresponding voltage values of the neutral density filters (from Oriel Co.) through the stoppedflow system. For this purpose, the fixed wavelength technique was used: the center of scan of the scanning monochromator was set at 526 nm, and the nutation set at zero. Then the same KMnO $_4$ solutions were successively pushed through the mixing cell of the stopped-flow apparatus. Their respective

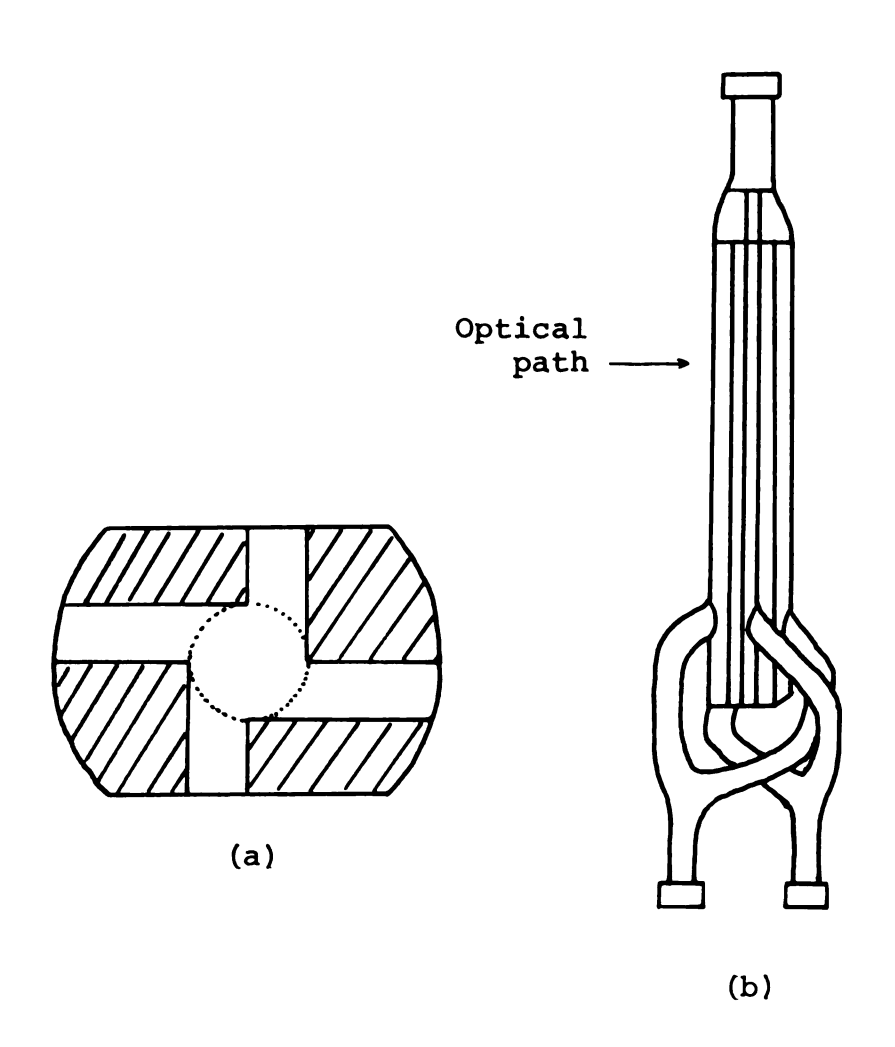


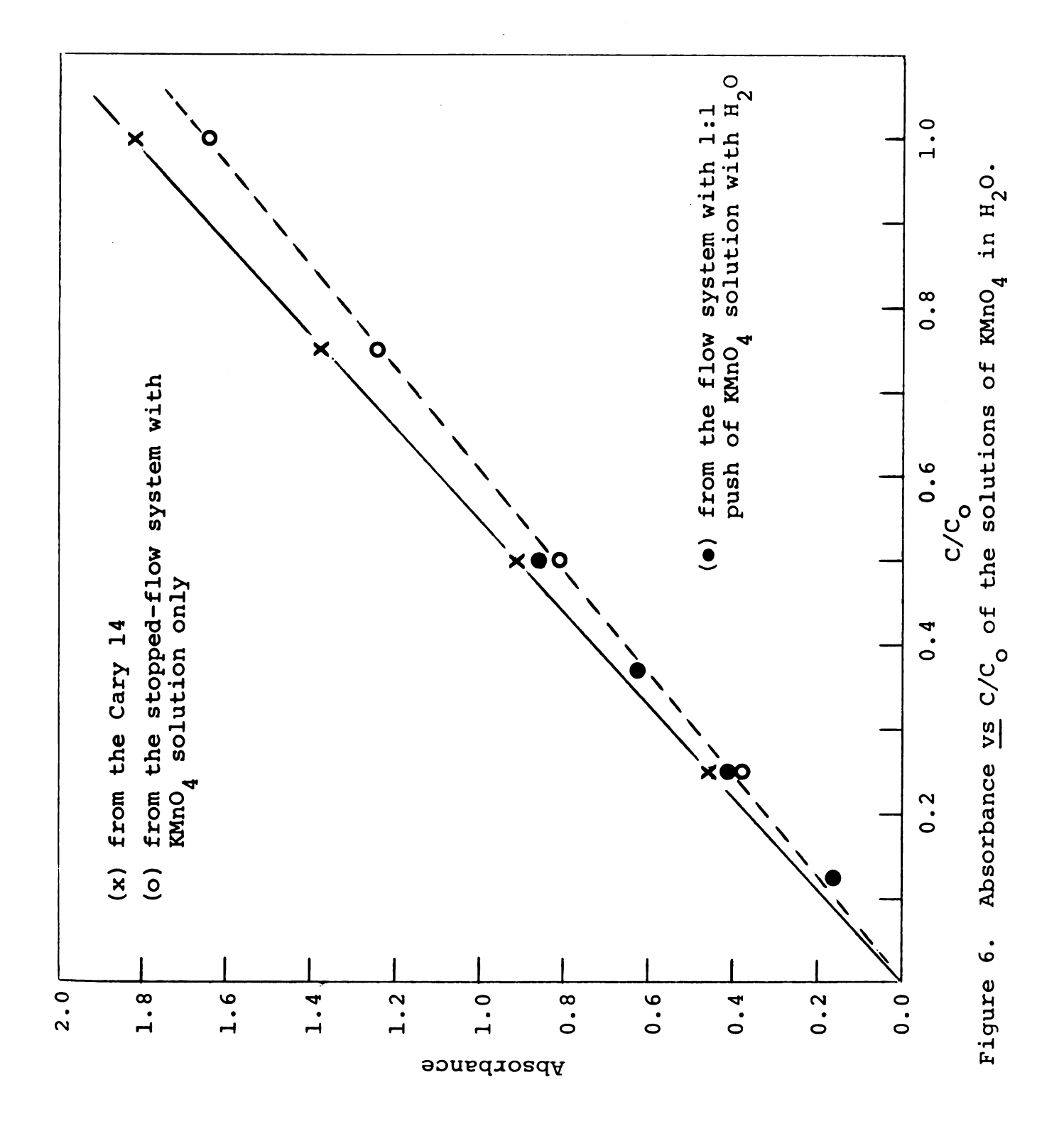
Figure 5. Four-jet mixing cell: (a) cross-section (b) entire flow cell.

absorbances were recorded by the digital voltmeter as voltage values. A calibration curve of the voltages obtained for the neutral density filters was then used to convert voltage values to absorbance values of the various KMnO_4 solutions recorded through the stopped-flow device. The plots of Absorbance from the Cary 14 and the Absorbance from the digital voltmeter $\underline{\mathrm{vs}}$ KMnO_4 concentrations give two straight lines (Figure 6). From the values of their slopes, an effective path length of the mixing cell of (0.90 + 0.02) mm was obtained.

From the fixed wavelength data, the effective stopping time of the stopped-flow system was estimated to be at most 5 msec.

3.5.4--Operations

After the entire stopped-flow apparatus had been pumped to a pressure of 1 x 10⁻⁵ torr, the stopcocks connecting the flow system to the vacuum line were shut off. Solutions of various reactants were let into the mixing vessels through the pair of burettes. The stopcocks A and B were opened; the pushing block which held the two pushing plungers was pulled downward with a lever. This allowed the solutions to flow from the mixing vessels into the two syringes on the bottom. Then the stopcocks A and B were closed and the stopcocks C and D were opened. The pushing block was pushed upward very rapidly by a manual pushing lever. The solutions were thus forced to mix and were permitted to react in the mixing cell,



and the resulting product solution flowed into the stopping syringe. When the stopping plunger hit the stopping plate, the flow of liquid was suddenly stopped, marking the end of a typical push and the beginning of the acquisition of useful rate data.

3.5.5--Data Acquisition

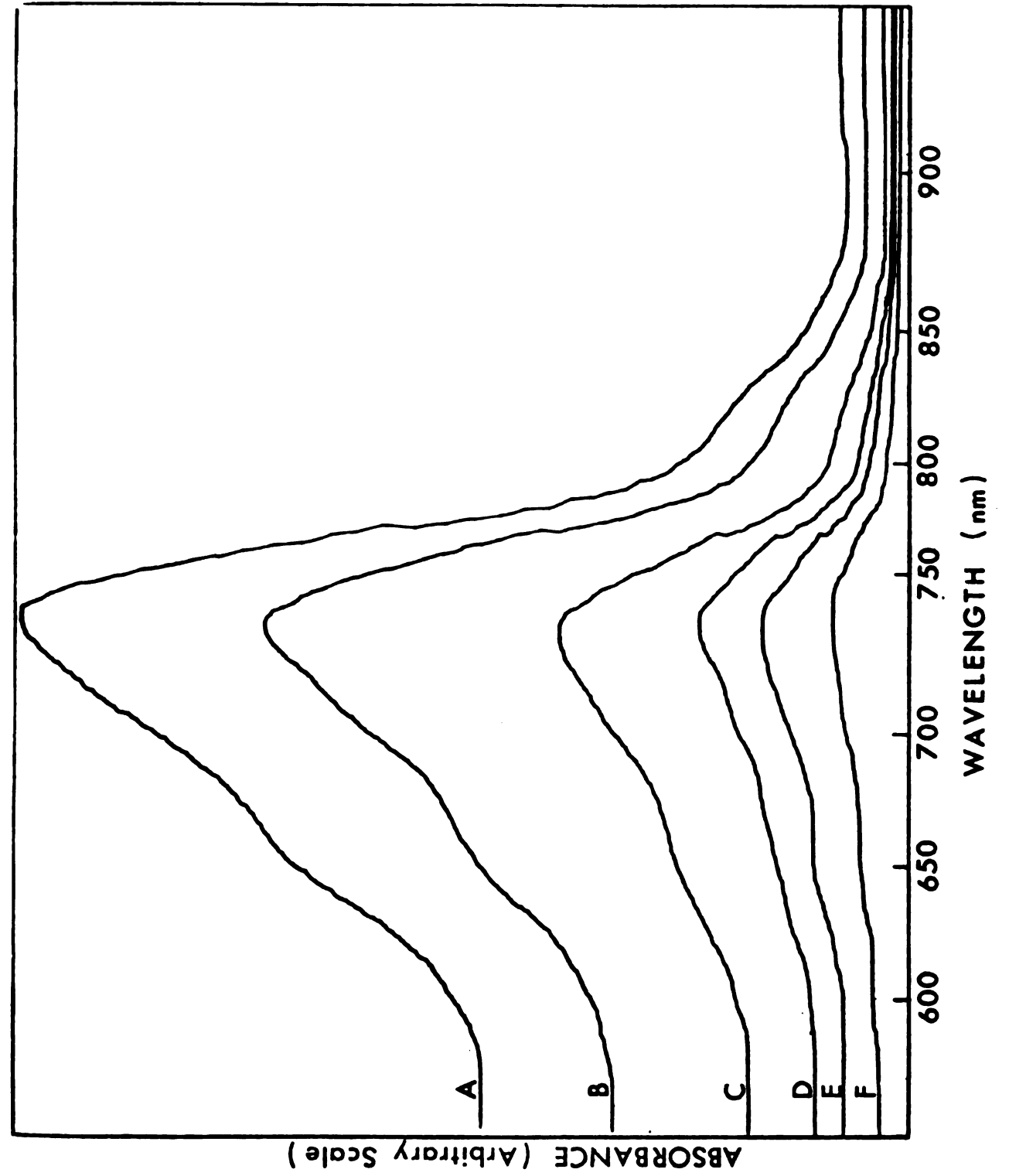
The decay of the spectrum of potassium anthracenide

(Figure 7) was followed spectrophotometrically. A schematic

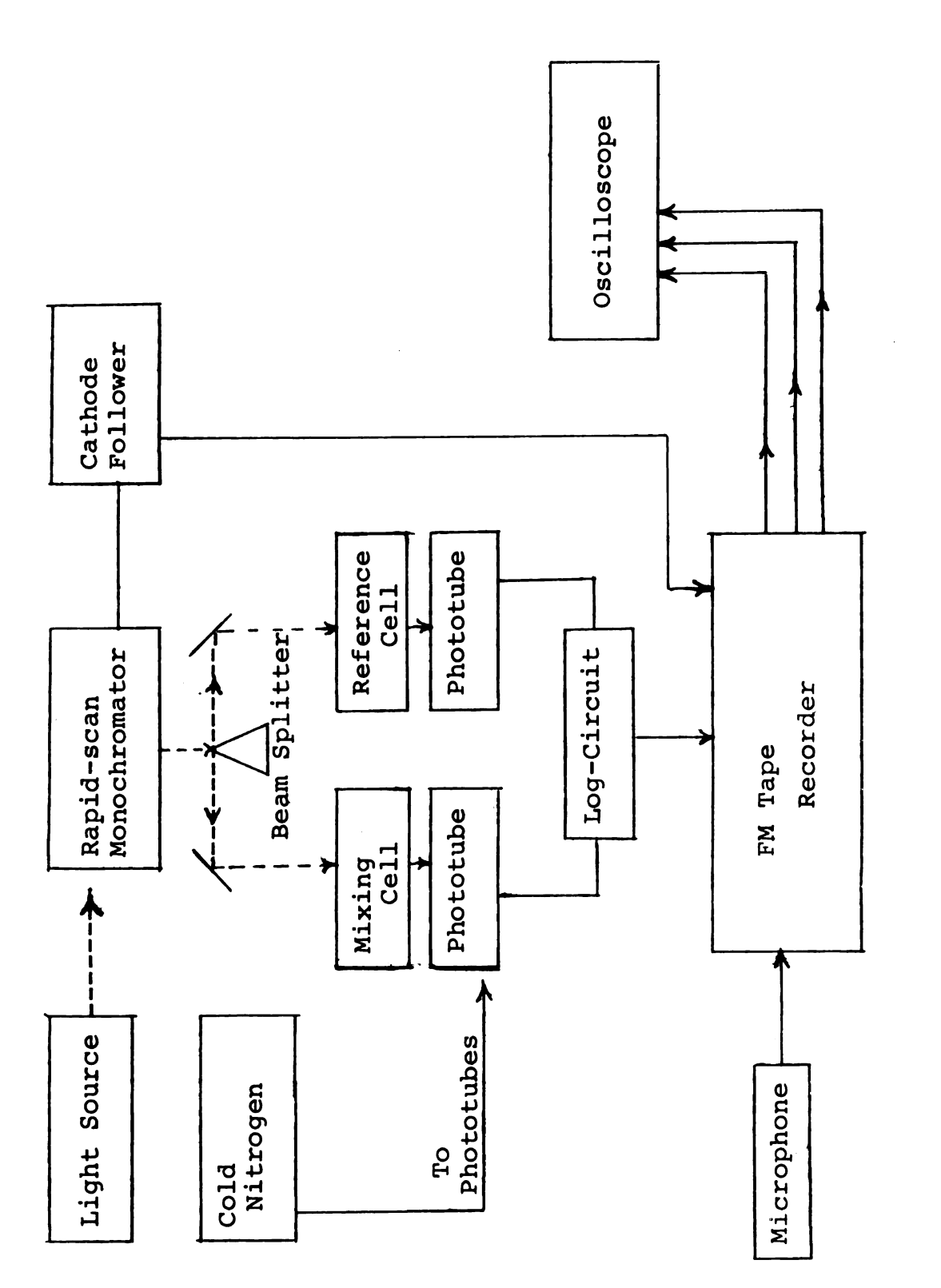
of the system for data acquisition is shown in Figure 8.

Light from an appropriate light source was scanned by a scanning monochromator over a desired range of wavelength before being split into two matched beams by a beam-splitter. The output light beams then passed through a reference cell or the mixing cell before striking the photomultipliers. A dual-log-circuit which employed a differential amplifier and Philbrick SPL-A operational amplifier received the output currents from the two multiplier phototubes and converted transmittance to absorbance. An FM tape recorder (Ampex SP-300) stored in four independent channels absorbance signals from the log circuit, trigger signals from the monochromator, verbal explanations from a microphone and a blank signal for later common-mode noise rejection. An oscilloscope connected to the FM tape recorder allowed signals to be monitored during the entire experiment.

Since in this study, the wavelength range of interest extended from 400 to 900 nm, the only light source used was a



Decay of spectrum of K An during reaction with EtOH in THF. Figure 7.



Block diagram of the data-acquisition system. Figure 8.

Bausch and Lomb tungsten-iodine lamp. The monochromator, a

Perkin-Elmer Model 108 Rapid-Scan Monochromator has a scanning
capability of from 3 to 150 scans per second over any wavelength region within the range of the quartz prism, provided
that the appropriate light source and detector are used.

Its detailed description has been given by Feldman (55). It
is no longer commercially available. Often a scanning rate
of 60 scans per second was high enough to permit one to observe a complete absorption spectrum of potassium anthracenide
during reaction. For very fast reactions, the scanning
technique was replaced by a fixed wavelength technique. In
this case, the motor of the scanning monochromator was stopped
and a desired single wavelength corresponding to a particular
peak position of the anion spectrum could be chosen.

In the fixed wavelength case, a trigger signal was produced every time the plunger hit the stopping plate. When the scanning technique was used, a special device described by DeBacker (56) produced the trigger signals in the following way. A slotted wheel attached to the drive mechanism of the monochromator let the light from a small neon light bulb hit a CdS photocell once per rotation of the mirror. A trigger signal of about 1 volt in 1 millisecond was thus produced at the beginning of each scan. This trigger signal was passed into the FM tape recorder through a cathode follower. Prior to the second series of experiments, the neon light bulb and the CdS photocell were repositioned by R. B. Coolen and

N. Papadakis behind a reflecting gear tooth of the metallic gear which drives the mirror.

The stacked-mirror beam-splitter was of the type used in the Bausch and Lomb Spectronic 505 Spectrophotometer. Spherical mirrors of 98 mm focal length (from Karl Lambrecht Co.) focused the two light beams onto the mixing cell and the reference cell respectively.

Two types of RCA photomultipliers were used, depending on the wavelength region of interest: an RCA 6199 for the region between 400 and 600 nm and an RCA 7102 for the region between 600 and 900 nm. It was necessary to set up a cooling system for the RCA 7102 phototubes to reduce thermal noise. Nitrogen gas passed through liquid nitrogen via copper tubing was used for this purpose.

Prior to each run, the two currents from the photomultipliers had to be matched by adjusting the input light received by each phototube. Also the linearity of the absorbance readings from the log-circuit was checked by using neutral density-filters (from Oriel Co.). The log-circuit was built with the following units purchased from Philbrick Research Inc.: a power supply PR-30C, a high impedance input amplifier P25A, a dual logarithmic transconductor Pll-P and an operational output-amplifier P65AU.

The tape recorder was an Ampex SP-300 FM Direct Recorder/
Reproducer. Finally, a Tektronix 564 Storage Oscilloscope
with a Type 2A63 Differential Amplifier Unit and a 3B4 Time

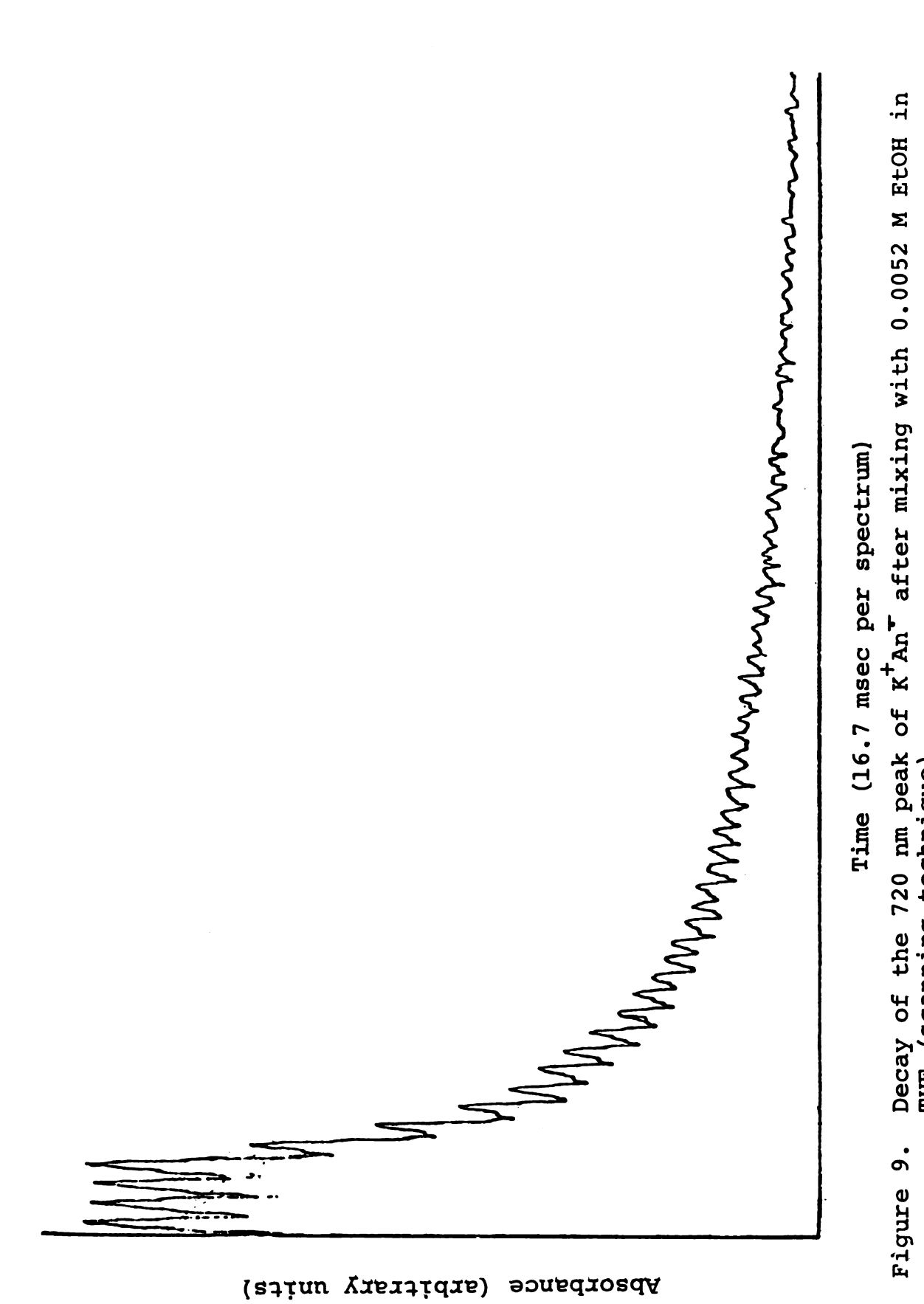
Base Unit served as a monitor.

3.5.6--Data Analysis

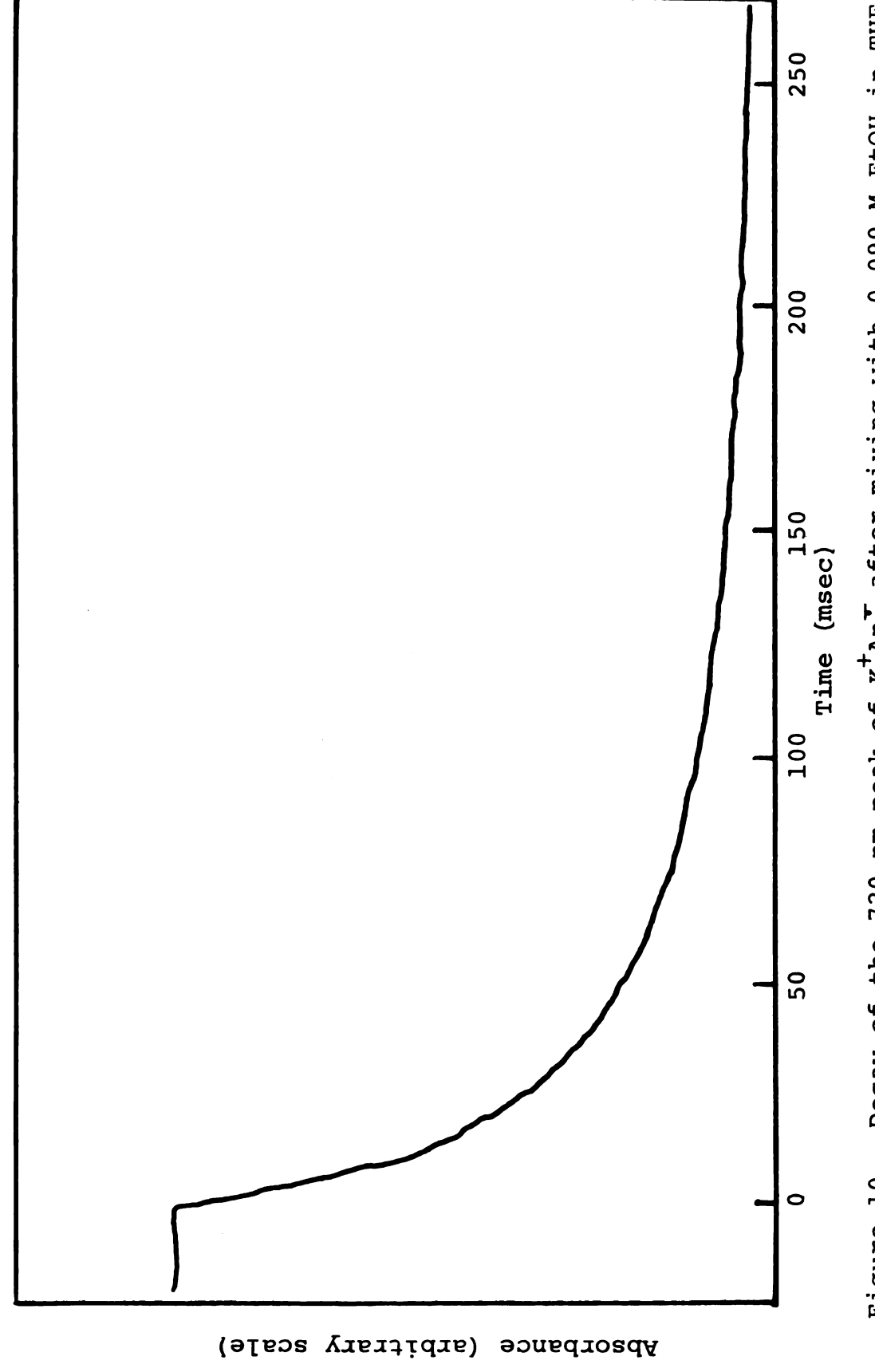
3.5.6.1--General

After the kinetics data had been properly stored on magnetic tapes as voltage fluctuations, the next problem was their analysis.

With the aid of a Computer of Average Transients (CAT), the kinetics data could be read from the tape recorder onto graph paper in analog form for display purpose, and onto computer cards in digital form for the purpose of rigorous analysis. Typical displayed data in analog form are shown in Figures 9 and 10. These graphs correspond to scanning and fixed wavelength techniques respectively. When the scanning technique was used, a series of spectra was recorded during an entire push. In this way, each spectrum after the flow stops is a decayed form of the preceding one. The basic idea, then, is to sample in digital form identical portions of the spectrum from successive spectra and to use a computer program to study them. A Varian C-1024 Computer of Average Transients (CAT) was used to produce the digital record. This small computer has 1024 channels, each of which can be independently triggered from an external trigger source. CAT can convert absorbance data stored on magnetic tape (as voltage versus time) into digital words which are stored in successive channels. A diagram of the analysis system is



Decay of the 720 nm peak of K^+An^- after mixing with 0.0052 M EtOH in THF (scanning technique). Figure 9.



Decay of the 720 nm peak of K⁺An⁻ after mixing with 0.090 M EtOH in THF (fixed wavelength technique). Figure 10.

shown in Figure 11. In order to better understand this somewhat complex network, let us give an example.

Suppose that we wish to study the decay of the 720 nm peak of the potassium anthracenide spectrum as a function of time. We then want to store a small portion of the 720 nm peak of each spectrum in 8 channels. In this way, 64 successive decay peaks will occupy the first 512 channels of the CAT. In order to implement this idea, it is necessary to use a pulse-delay unit. Although a trigger signal is produced at the beginning of each spectrum, the pulse-delay device can delay this trigger signal for any desired time. This delayed trigger signal can be used to produce 8 square-wave pulses from a waveform generator. These pulses command the CAT to successively open 8 channels for data storage. The frequency of the waveform generator determines the time-interval between consecutive pulses. The next 8 channels of the CAT will be triggered by the next delayed trigger, and so forth until all 512 channels are filled. Thus absorbance values of the first 64 spectra sampled at 8 different wavelengths were stored in the CAT, ready to be punched onto computer cards for analysis.

For more specific details refer again to the diagram in
Figure 11. The absorbance signal and the signal from the blank
channel of the tape recorder were sent through a variable gain
differential amplifier to reduce common mode recorder noise.

A Tektronic Storage Oscilloscope displayed the output waveform
for monitoring purposes and this analog voltage was also

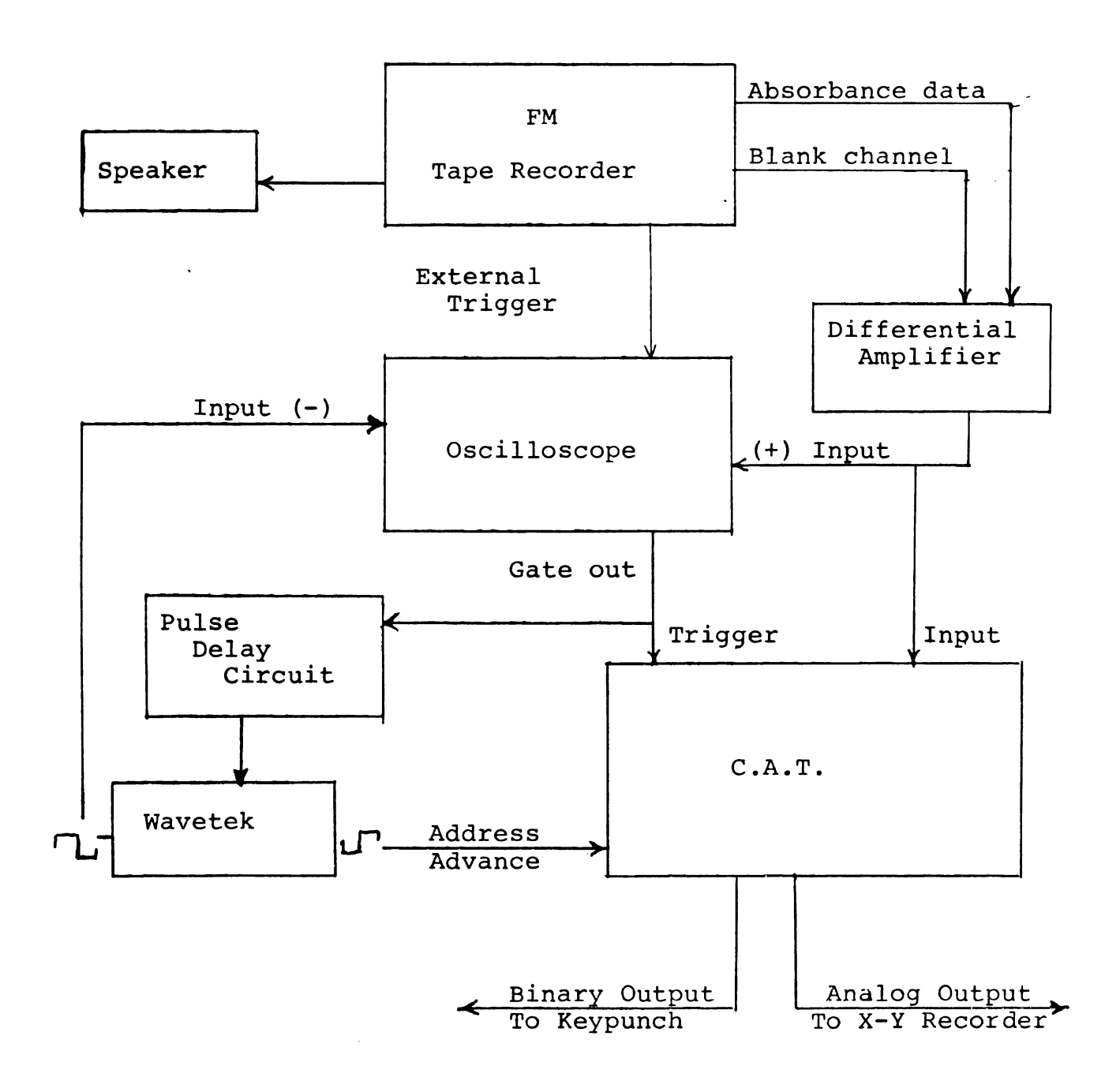


Figure 11. Block diagram of the analysis system.

connected to the input of the CAT. The pulse-delay unit received gated trigger pulses from the oscilloscope and sent the delayed signals into a Wavetek Model 116 Signal Generator. This waveform generator produced square-waves which were sent into the channel advance input of the CAT and also into the second channel of the differential input amplifier of the oscilloscope. In this way, we could follow on the oscilloscope screen not only the entire spectrum but also which portions of the absorption spectrum were being stored in the CAT in digital form. After acquisition of the data, they could be punched onto computer cards by an IBM type 526 Keypunch which was coupled to the CAT by a Varian C-1001 coupler.

Simultaneously, analog plots of the data could be obtained.

Two computer programs, PUNDAT and KINFIT were then used with a CDC-6500 computer to analyze those kinetics data.

When the fixed wavelength technique was used to collect the data, the pulse-delay circuit and the Wavetek were not needed in the analysis system.

3.5.6.2--Program PUNDAT

The data obtained from the CAT had to be transformed into a form acceptable to program KINFIT, the main tool for data analysis. Program PUNDAT was written for this purpose by Dr. V. A. Nicely. It was modified later by Dr. E. R. Minnich. A detailed description of this program was given in Reference 48.

3.5.6.3--Program KINFIT

This program was written by Nicely and Dye and is described in detail elsewhere (48,57,58). Although program KINFIT cannot decide whether a given rate law is suitable for a particular set of data, it gives the following information:

- the best estimates of the parameters obtained from a least-squares treatment of the data;
- the sum of the squares of the residuals;
- the multiple correlation coefficients and the variance-covariance matrix;
- the comparison between calculated and experimental values;
- a print-plot of calculated and observed values.

Having all the above information, an experienced program user can decide whether to accept or to reject the trial rate law.

IV. SURVEY AND TREATMENT OF THE DATA

As mentioned in the Introduction, this study is a continuation of Minnich's work. However, instead of continuing to examine various aromatic hydrocarbons and numerous alcohols in tetrahydrofuran (THF) and dimethoxyethane (DME), we chose only one system. This study deals with the protonation of potassium anthracenide (K⁺An⁻) with ethanol in THF over a wide concentration range of ethanol and of anthracene. We also used dicyclohexyl-18-crown-6 (crown) to test the effect of ion-pairing on the protonation rate.

4.1--Survey and Discussion of the Data

There were two main series of experiments as shown in Table I. In the first series, the initial concentration of the $K^{\dagger}An^{\dagger}$ stock solution in THF was rather low ($\sim 2 \times 10^{-4}$ M after mixing). The reason was that, through inexperience, we did not spread the mirror of potassium metal over a large area on the glass walls of the reaction vessel (Figure 2b). Therefore, the anthracene solution did not react with enough potassium metal to produce a sufficiently concentrated $K^{\dagger}An^{\dagger}$ solution. In certain runs of this series, we could not analyze the collected data for one of the following reasons:

TABLE I List of Experiments

Comments				reconnique Too fast		Too slow		decay Too much background noise								
[An] M	6.2×10^{-4}	8.3 x 10 ⁻⁴	8.3 x 10 ⁻⁴	6.2×10^{-4}	6.2×10^{-4}	6.4×10^{-4}	6.4×10^{-4}	6.4 x 10-4	1.7×10^{-3}	1.6 x 10 ⁻³	1.5 x 10 ⁻³	1.5 x 10 ⁻³	9.9 x 10 ⁻³	1.0 x 10 ⁻²	2.5 x 10 ⁻²	
[EtOH] M	8.7 x 10 ⁻³	8.7 x 10 ⁻³	6.6 x 10 ⁻¹	6.6 x 10 ⁻¹	1.3 x 10 ⁻¹	8.8 x 10 ⁻³	6.6 x 10 ⁻¹	6.6 x 10 ⁻¹	4.5 x 10 ⁻³	8.6 x 10 ⁻²	1.5 x 10 ⁻³	2.4×10^{-3}	2.1 x 10 ⁻³	4.2 x 10 ⁻³	3.5 x 10 ⁻³	
[Crown] _O M	1	1	!	!	1	4.0×10^{-4}	4.0 x 10 ⁻⁴	1	1	1	1	i	1	1	!	
Scans/sec	09	09	120	120	120	09	60-120	fixed λ	09	fixed λ	60-120	120	120	120	120	
Run	1-A	1-B	1-c	1-D	1-E	1-F	1-G	1-н	2-A	2-B	2-C	2-D	2-E	2-F	2-G	

						Slow pseudo first-order		rollowed by slow ilrst- order decay	
2.5 x	4.3 ×	4.4 x	4.4 x	2.0 x	2.4 x	1.2×10^{-3}	1.9×10^{-3}	1.9×10^{-3}	
3.8 x 10 ⁻²	1.5 x 10 ⁻³	4.5 x 10 ⁻¹	8.6 x 10 ⁻²	8.9×10^{-2}	4.5 x 10 ⁻¹	4.5 x 10 ⁻¹	4.5 x 10 ⁻¹	2.3 x 10 ⁻¹	
ł	!	1	1	1	1	1.9 x 10 ⁻³	7.7×10^{-4}	7.7×10^{-4}	
120	09	fixed λ	fixed λ	fixed λ	fixed λ	09	fixed λ	09	
2-н	2-3	2-K	2-L	2-M	2-N	2-0	2-P	2-0	

- the reactions were too fast for the scanning technique (high ethanol concentration, no crown);
- the reactions were too slow (low EtOH concentration, with crown);
- there was too much background noise for the fixed wavelength technique because of low absorbance.

The majority of the data come from the second series of experiments. This time, we wanted to have a high enough concentration of $K^{\dagger}An^{\dagger}$ to work with easily. In fact, we were so careful in spreading out the active surface of K metal on the glass walls that we almost overshot the desired initial $K^{\dagger}An^{\dagger}$ concentration ($\sim 2.4 \times 10^{-3}$ M after mixing).

Besides these two main series of experiments, we reanalyzed most of Minnich's data. In fact, Minnich did a great
deal of screening work, and obtained many data on a variety
of systems. However, in most cases he analyzed only a few
pushes at each concentration in order to test various mechanisms. The reader will see later that we needed nearly all
of Minnich's data for the THF solvent system in order to
distinguish between several proposed mechanisms. This need
became apparent only after completion of our study. A summary
of Minnich's data as re-analyzed is shown in Table II.

4.2--Data Treatment

In conducting this study, we had three main purposes in mind:

TABLE II

List of Minnich's Experiments Re-analyzed by the Author

(2K⁺An⁻ + 2ROH THF AnH₂ + An + 2K⁺RO⁻)

Run	ROH	Range of ROH concentrations (M)	Number of ROH concentrations
KR7,5-6	EtOH	$(4.32-2.20) \times 10^{-3}$	2
KR9,11-14	EtOH	$(5.0-0.48) \times 10^{-3}$	4
KR7,1-4	н ₂ 0	$(3.6-0.38) \times 10^{-1}$	4
KR8,4-5	н ₂ 0	$(2.2-0.8) \times 10^{-1}$	2
KR9,9-10	н ₂ 0	$(4.7-0.41) \times 10^{-2}$	2
KR10,1-3	i-PrOH	$(1.14-0.11) \times 10^{-1}$	3
KR10,4-6	t-BuOH	$(2.0-0.54) \times 10^{-2}$	3
KR10,7-9	MeOH	$(3.7-0.5) \times 10^{-3}$	3

- a) to reconfirm the existence of a second-order protonation of potassium anthracenide in THF;
- b) to test the ion-cluster mechanism (Equations 42, 43) and the dianion mechanism (Equations 47, 48) over a wide range of concentrations of ethanol and anthracene. The ethanol concentration was varied from a very high value (~ 0.5 M) down to a value less than the initial concentration of K⁺An⁻. In addition the concentration of free anthracene was also varied from an upper limit of ~ 0.04 M to a concentration which was less than that of K⁺An⁻.
- c) in case these proposed mechanisms failed to fit our experimental data over the entire concentration range, search for new mechanisms.

Simultaneously, a number of attempts were made to fit the data at different concentrations directly to a particular mechanism. However, only three or four pushes could be examined at a time and this procedure was not successful. Therefore, the data (without crown) were fit to a pseudo parallel first—and second—order rate law where possible. The integrated form of the following differential rate law:

$$-\frac{d[K^{+}An^{+}]}{dt} = k_{ps}[K^{+}An^{+}]^{2} + k_{ps}[K^{+}An^{+}]$$
 (53)

was fit to the data by using a non-linear least-squares program (57). Usually when [EtOH] and [An] were appreciably higher than $[K^{+}An^{-}]$, the data were well-described by this

rate law. A representative fit of this rate law to our data is given in Figure 12. The first-order contribution to the decay of the absorbance only became appreciable above [EtOH] % 0.1 M. In those cases for which [EtOH] and [An] were comparable to $[K^{+}An^{-}]$, pseudo order kinetics were no longer valid. For these cases, we fit the data by using the equation:

$$-\frac{d[K^{+}An^{-}]}{dt} = \left(\frac{2k_{+}}{\frac{k_{-}[An]}{k_{1}[ROH]}}\right) [K^{+}An^{-}]^{2}$$
 (54)

derived from the dianion mechanism:

$$2(An^{-},K^{+}) \xrightarrow{k_{+}} (An^{-},2K^{+}) + An$$
 (55a)

$$(A_n^-, 2K^+) + ROH \xrightarrow{k_1} K^+A_nH^- + K^+RO^-$$
 (55b)

$$K^{+}AnH^{-} + ROH \xrightarrow{fast} AnH_{2} + K^{+}RO^{-}$$
 (55c)

with the assumption that a steady-state concentration of $(An^{=},2K^{+})$ was achieved. For these data, the KINFIT program was used in its differential form. For comparison with the data at higher concentrations, the "pseudo second-order rate constant" was obtained from:

$$k_{ps} = \frac{2k_{+}}{\frac{k_{-}[An]}{1 + \frac{k_{-}[ROH]}{[ROH]}}}$$
(56)

In this case, [An] and [ROH] must be adjusted to their values

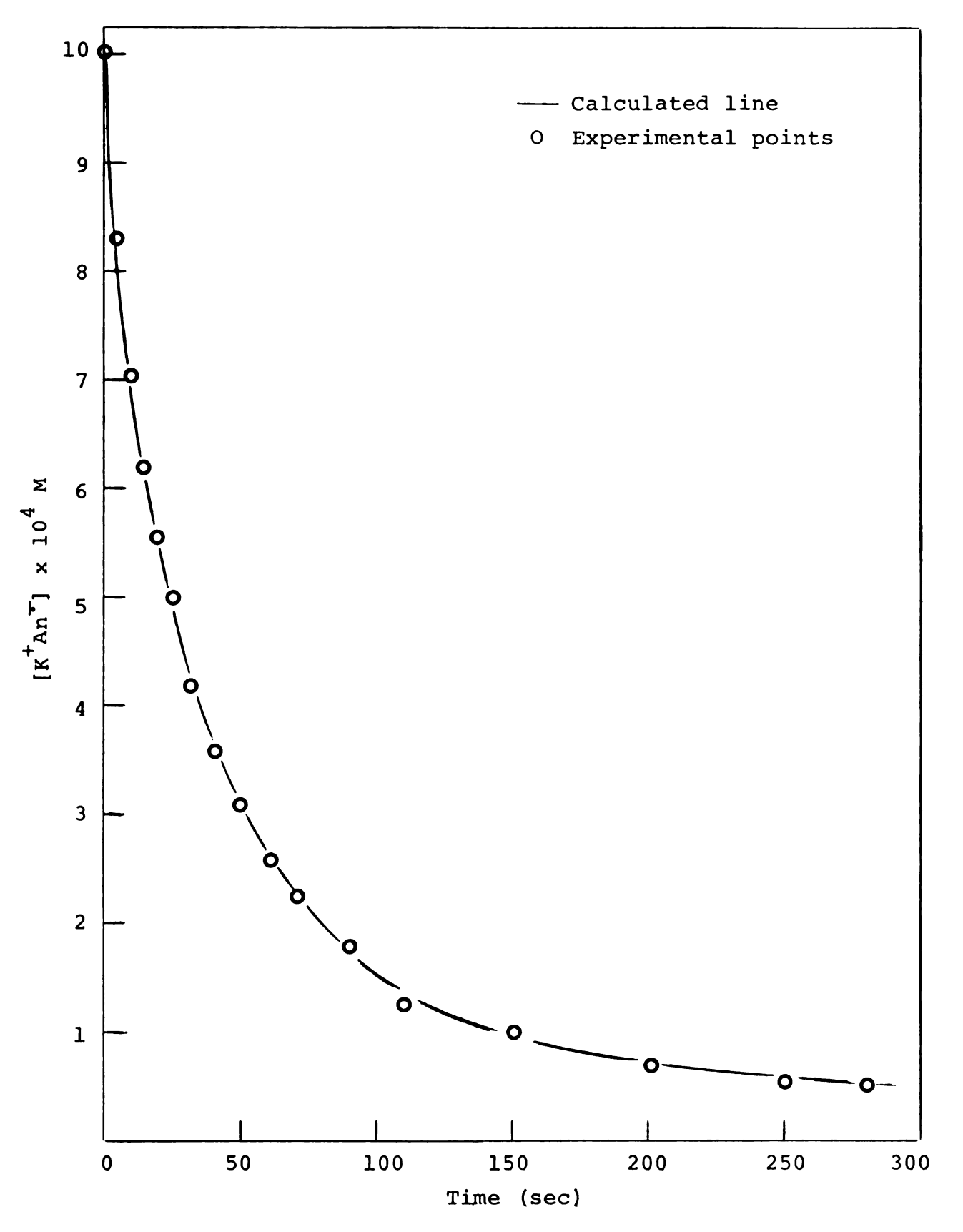


Figure 12. Parallel first- and second-order kinetics applied to the reaction $K^{+}An^{-}$ + EtOH in THF ([EtOH] = 8.9 x 10^{-2} M).

at the point at which k_{ps} is to be calculated. The values of [An] and [ROH] were calculated from the mass balance equations:

$$[An]_{t} = [An]_{0} + \frac{1}{2} ([K^{+}An^{-}]_{0} - [K^{+}An^{-}]_{t})$$
 (57)

$$[ROH]_{t} = [ROH]_{o} - ([K^{+}An^{-}]_{o} - [K^{+}An^{-}]_{t})$$
 (58)

It was necessary to use this procedure because at low concentrations of ROH, the second-order rate constants are sensitive to variations in the ratio [ROH]/[An]. By this procedure, we found that the dianion mechanism fits our data well at low [EtOH] (<0.01 M). In addition, by using this procedure it was possible to calculate the values of the rate constants not only at the initial point of a decay curve, but also at any point along this curve. In one extreme case, for which [EtOH] was less than [K⁺An⁻], neither the pseudo parallel first- and second-order rate law nor the dianion mechanism could be used to fit the data. For this case, we used the empirical rate law:

$$-\frac{d[K^{\dagger}An^{\dagger}]}{dt} = k[ROH][K^{\dagger}An^{\dagger}]^{2}$$
 (59)

with the mass balance equation (58) to fit the data over only the first half-life of the reaction. For this case, of course,

$$k_{ps} = k[ROH]$$
 (60)

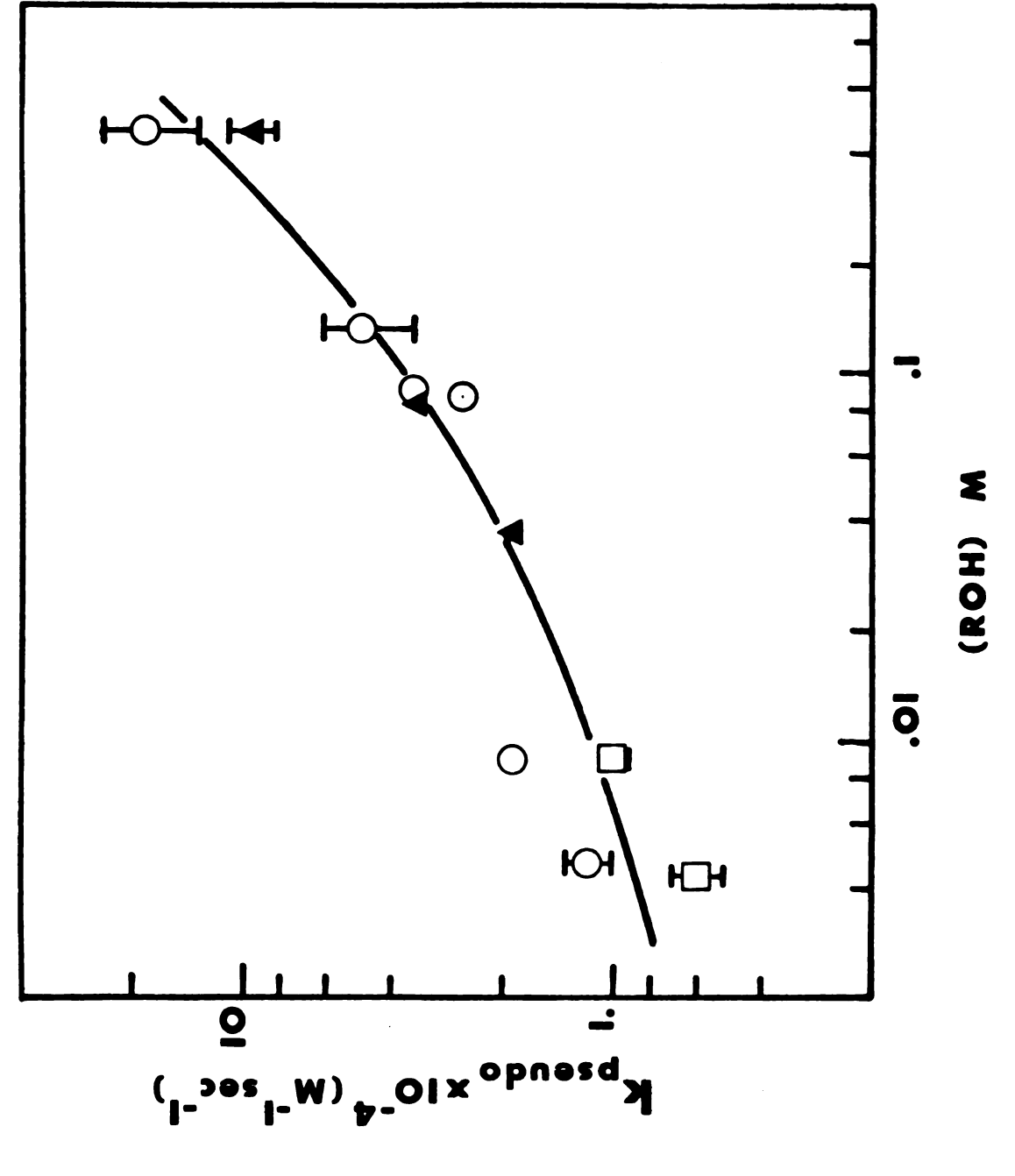
By these procedures, it was possible to obtain values of $k_{\rm ps}$ (2nd) for all cases. This proved to be a valuable aid in testing new mechanisms.

V. RESULTS AND CONCLUSIONS

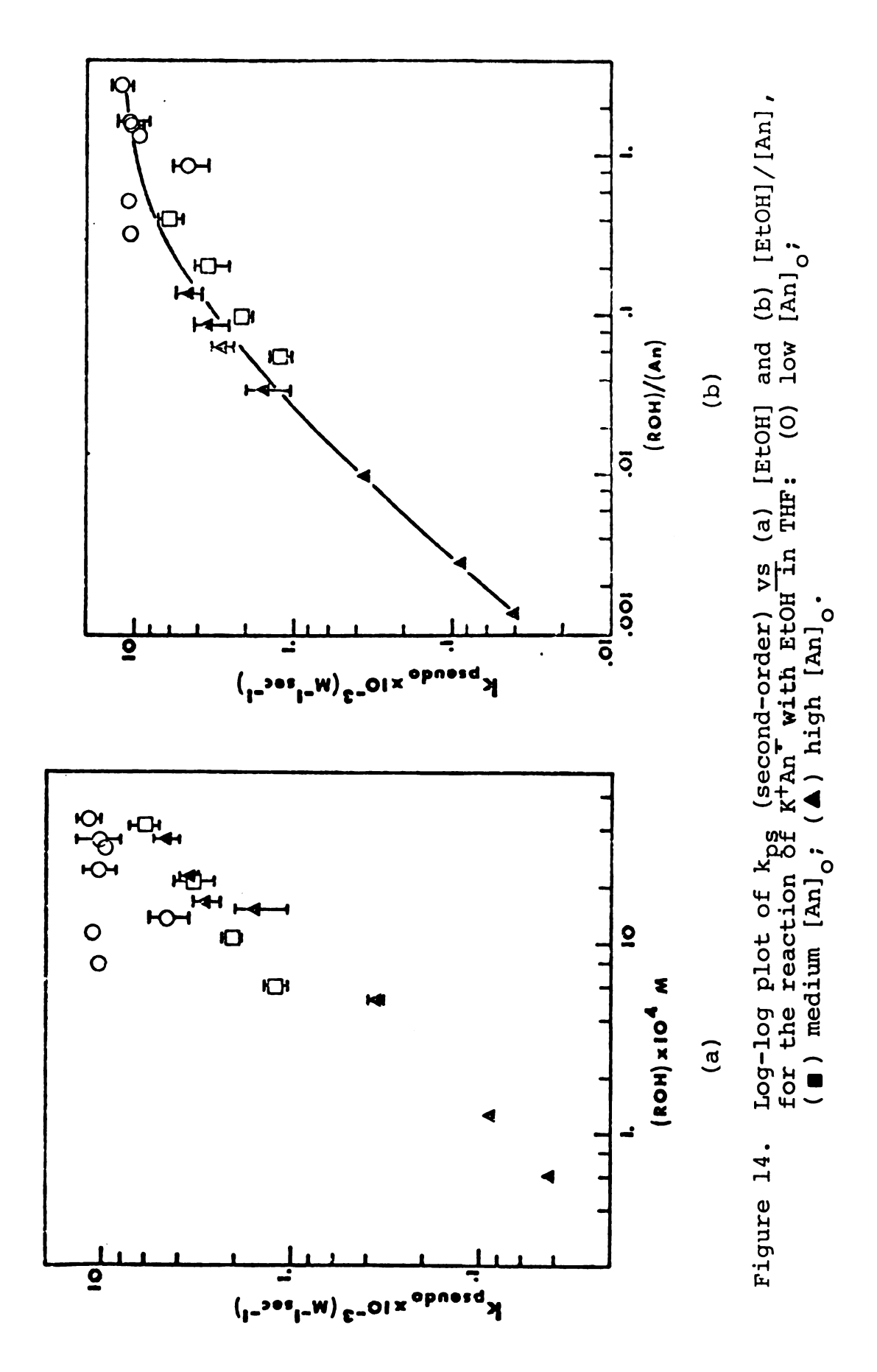
5.1--Results

5.1.1--Inapplicable Mechanisms

As mentioned in the last chapter, one of our goals was to test the ion-cluster mechanism (Equations 42, 43) and the dianion mechanism (Equations 54, 55). In fact, both mechanisms predict that the pseudo second-order protonation rate constant would reach an upper limit set by k_{+}^{1} and k_{+} respectively, and become independent of [EtOH] at high ethanol concentrations. This did not happen in our case: the rates continued to increase as the ethanol concentration was increased as shown in Figure 13. Figure 13 also shows that the rates become less sensitive to the anthracene concentration at high [EtOH]. Clearly neither the dianion mechanism nor the ion-cluster mechanism alone can fit the data at high [EtOH]. On the other hand, for low [EtOH] ($\stackrel{\mbox{\tiny def}}{\sim} 0.01 \mbox{\scriptsize M}$), the diamion mechanism fits the data well, while the ion-cluster mechanism failed to predict the observed effect of [An] on the protonation rate. Figures 14a,b show the superiority of the former mechanism over the latter: while the plot of k_{ps} (2nd) \underline{vs} . [ROH] displays scattered data points which correlate with [An], the same values of k_{ps} (2nd) when replotted \underline{vs} , [ROH]/ [An] show a more ordered trend of variation.



Lqg-log plot of k (second-order) vs [EtOH] for the reaction of K An with EtOH in THF: (0) low initial free An concentration; () medium initial [An]; () high initial [An]. Figure 13.



5.1.2--Effect of Crown

The effect of solvent on the rate of protonation has been reported in the literature (48,49,50,52). When the formation of contact ion-pairs is not favored, the protonation rate is markedly lower. In order to test this effect of ion-pairing, we added dicyclohexyl-18-crown-6 (crown) (59), to a solution of $K^{\dagger}An^{\top}$ in THF prior to protonation. The crown compound has been proven to be a good complexing agent for alkali metal cations (60,61). ESR results indicate that crown breaks up the contact ion-pairs of $K^{\dagger}An^{\top}$. The effect on the protonation rate is dramatic. The addition of crown essentially wipes out the second-order protonation, provided that [crown] $R^{\dagger}An^{\top}$. Only a slow first-order component remains, as shown in Figure 15.

Although the studies with crown are only preliminary in nature, it is interesting to note that the first-order protonation rate of the solvent (and/or crown)-separated ion-pair, An | | K (in THF with excess crown) seems to be about 100 times smaller than the first-order protonation rate of the contact ion-pair, An , K (in THF without crown). In the intermediate case for which [crown] < [K An], the decay curve is broken into two portions: a fast initial decay followed by a much slower first-order decay as shown in Figure 16.

5.1.3--Proposed Mechanisms

We have seen that neither the diamion mechanism nor the ion-cluster mechanism fit our data over the entire range of

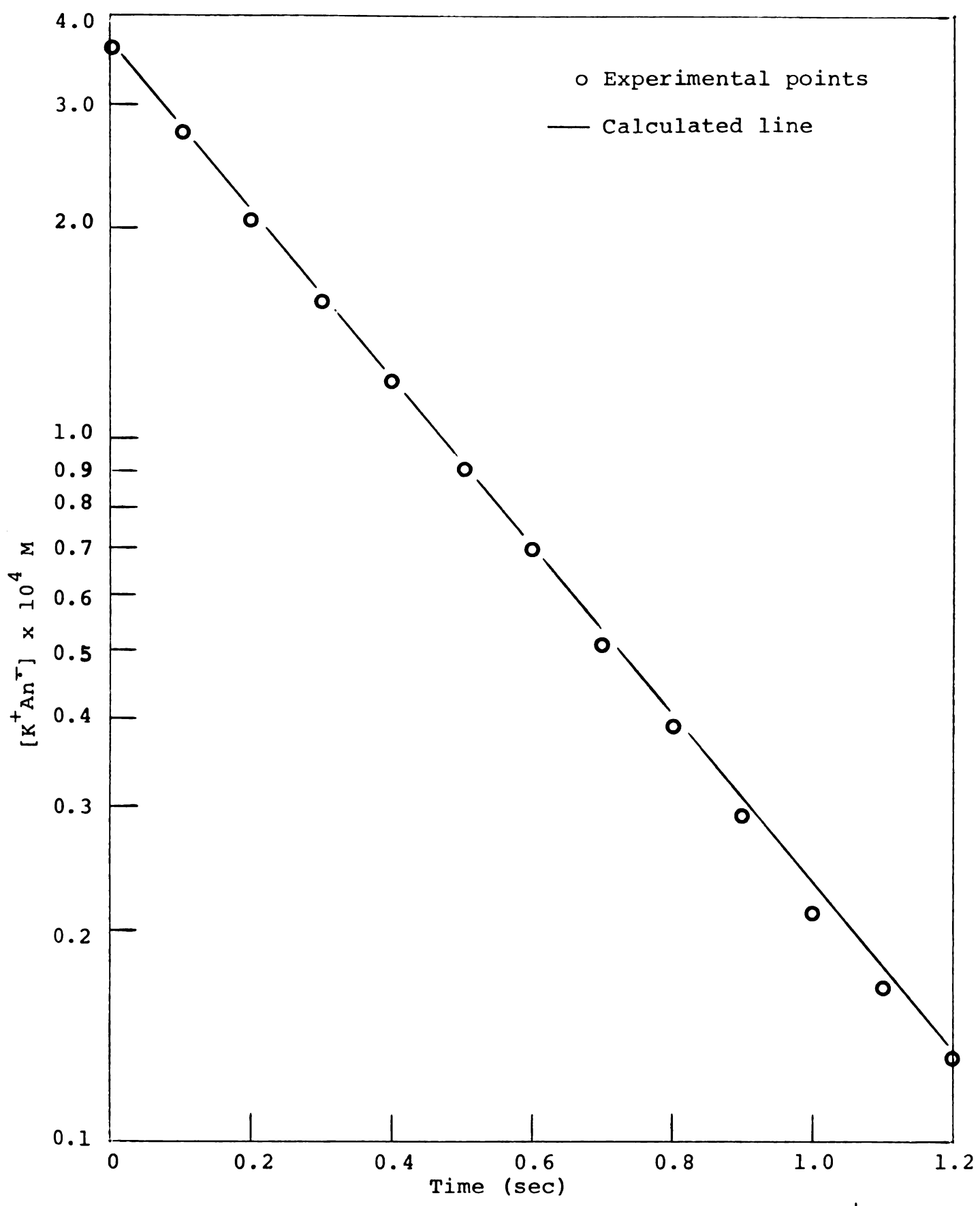
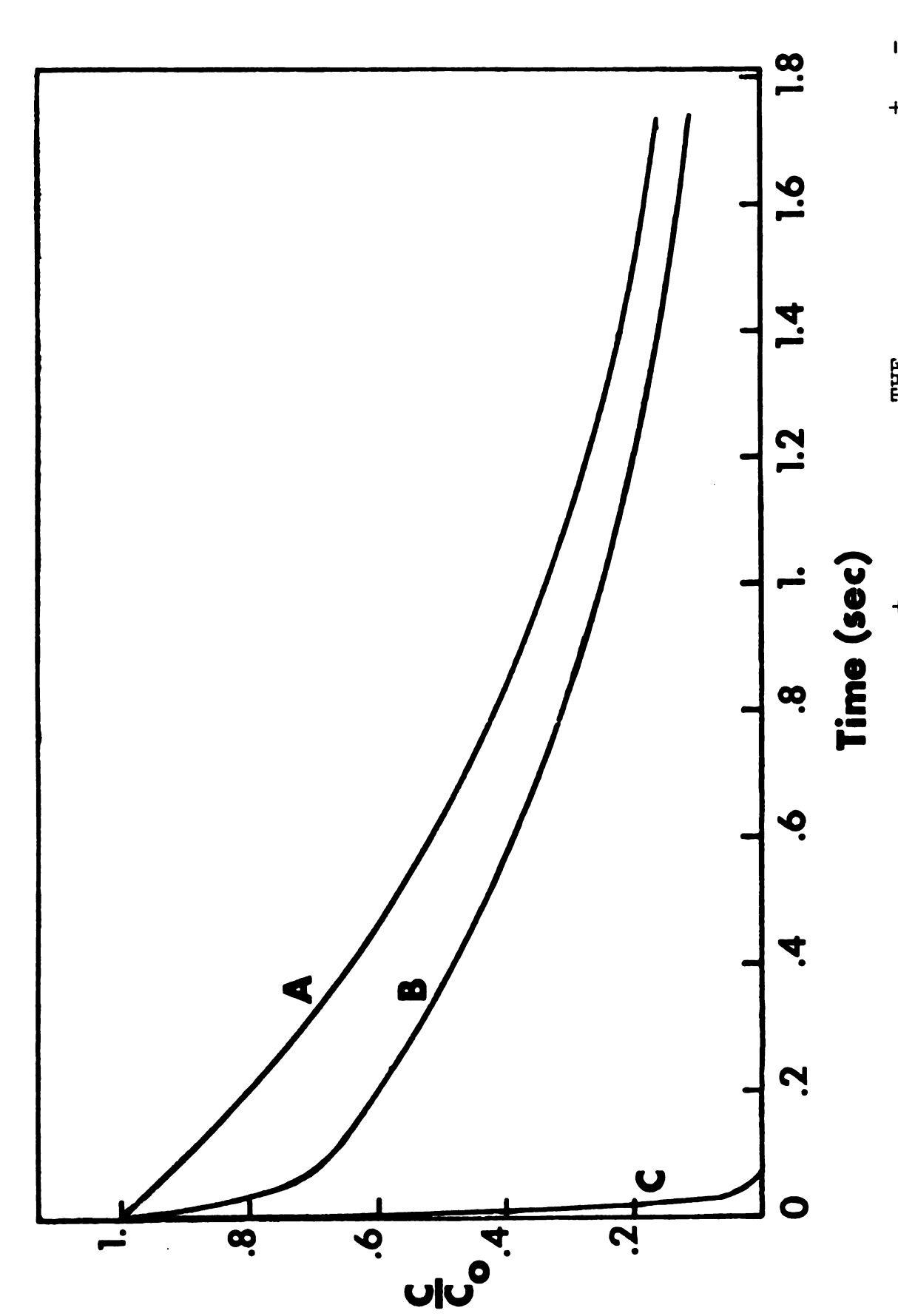


Figure 15. Pseudo first-order plot for the reaction of K⁺An⁻⁻ + (excess crown) with EtOH in THF.



 $C/C_0 \frac{vs}{vs}$ time for the reaction: $2K^+An^+ + 2EtOH \frac{THF}{TH^2} + AnH_2 + An + 2K^+EtO^-$:
(A) [Crown] > [K⁺An⁻]; (B) [Crown] < [K⁺An⁻]; (C) no Crown. $[EtOH]_O = 0.45 \text{ M for all cases.}$ Figure 16.

concentrations of EtOH and An. In the search for a new mechanism, we must take into account the three main effects already mentioned in part 5.1.1:

- the protonation rate continued to increase with increasing [EtOH];
- the rate at high [EtOH] did not depend significantly on the anthracene concentration;
- the diamion mechanism fit the data well at low [EtOH].

A suitable mechanism would seem to require the formation of the anthracene dianion $(An^{\pm}, 2K^{+})$ to account for the behavior at low [EtOH]. It also might include the formation of the ion-cluster $(An^{\pm}, K^{+})_{2}$ since the protonation of this species leads to a mechanism which does not depend on [An].

5.1.3.1.--Dianion and Ion-cluster Mechanism

For the reason given above, we tested the following mechanism:

$$2(An^{+},K^{+}) \xrightarrow{K_{Q}} (An^{+},K^{+})_{2} \xrightarrow{k_{+}^{"}} An^{=},2K^{+} + An$$
 (61a)

$$An^{-}, 2K^{+} + ROH \xrightarrow{k_{1}} K^{+}AnH^{-} + K^{+}RO^{-}$$
 (61b)

$$(An^{-}, K^{+})_{2} + ROH \xrightarrow{k_{2}} K^{+}AnH^{-} + K^{+}RO^{-} + An$$
 (61c)

$$K^{+}AnH^{-} + ROH \xrightarrow{fast} AnH_{2} + K^{+}RO^{-}$$
 (61d)

which leads to the general rate law:

$$-\frac{d[K^{+}An^{-}]}{dt} = \begin{bmatrix} \frac{2k_{+}^{"}K_{Q}}{k_{-}^{"}} & + 2k_{2}K_{Q}[ROH] \\ 1 + \frac{k_{-}^{"}}{k_{1}} & \overline{[ROH]} \end{bmatrix} [K^{+}An^{-}]^{2}$$
(62)

provided a steady-state concentration of the dianion (An = ,2K +) is reached.

At high values of [ROH], the second term of this rate law becomes predominant, and the decay becomes pseudo second-order in [K⁺An⁻] and first-order in [ROH] after correction for the first-order protonation. At low [ROH], the second term becomes less important and the rate expression reverts to that of the dianion mechanism.

An important point should be made here: the "solvent caged" complex (An , 2Na ; An) suggested by Szwarc and coworkers (52) cannot be kinetically distinguished from the ion-cluster species (An , K).

If the formation of the cluster involves only electrostatic forces, the value of the equilibrium constant for the reaction:

$$2An^{\top}, M^{+} \xrightarrow{K_{Q}} (An^{\top}, M^{+})_{2}$$
 (63)

can be estimated from the Fuoss expression (62,63):

$$\kappa_{Q} = \frac{N_{AV}}{2000} \left(\frac{\pi}{3}\right)^{3/2} \frac{\mu^{2}}{DkT} \frac{e^{Y}}{y^{7/2}} \left(\frac{1}{2\lambda^{2}} - 1\right)^{-1/2}$$
(64)

where: μ = dipole moment of the ion-pair An^{*},M[†] considered as an ellipsoid;

a = major axis of the ellipsoid;

 $\lambda a = minor axis$

and:

$$y = \frac{\mu^2}{(\lambda a)^3 DkT}$$
 (65)

Using the observed value of the ion-pair association constant of Na⁺An⁻ (64), we can calculate the value of <u>a</u> from the Fuoss equation for ion-pair formation (63):

$$K_{a} = \frac{4\pi a^{3} N_{AV}}{3000} e^{b}$$
 (66)

with

$$b = \frac{e^2}{aDkT}$$
 (67)

The value of <u>a</u> obtained this way is $\underline{a} = 5.7 \, \text{Å}$. From this value, we get $K_Q \simeq 48 \, \text{M}^{-1}$. Also the Fuoss-Krauss expression (65) for the equilibrium constant for triple-ion formation and the assumption that the equilibrium constant for the reaction:

$$An^{\dagger}, K^{\dagger}, An^{\dagger} + K^{\dagger} \Longrightarrow (An^{\dagger}, K^{\dagger})_{2}$$
 (68)

is the same as that for ion-pair formation, Equation 66, gives $K_Q \simeq 67 \text{ M}^{-1}$. Therefore, we can estimate a reasonable value of 50 M^{-1} for K_O .

Returning to the rate expression (62), we see that it contains 3 adjustable parameters, $k_{+}^{"}K_{Q}$, $k_{-}^{"}/k_{1}$ and $k_{2}^{}K_{Q}$ with strong coupling between them. We used a lot of computer time trying to couple various data sets and fit them directly to

Equation 62 in order to extract reasonably stable values of these three parameters. Finally, we realized that the separation of these strongly coupled parameters depends upon the use of many different values of [An] and [ROH]. This cannot be satisfied by coupling just a few data sets. Thus we decided to use an indirect approach as follows. We write Equation 62 as:

$$-\frac{d[K^{\dagger}An^{\dagger}]}{dt} = f(An,ROH)[K^{\dagger}An^{\dagger}]^{2}$$
 (69)

where:

$$f(An,ROH) = \frac{2k_{+}^{"}K_{Q}}{k_{-}^{"}[An]} + 2k_{2}K_{Q}[ROH]$$
(70)

depends upon [An], [ROH] and the 3 parameters. From the material balance equations (Equations 57, 58), we can get [An] and [ROH] at any point during the reaction. At high values of [ROH] and [An], f(An,ROH) is just the pseudo second-order rate constant. At low values of [ROH], f(An,ROH) is obtained from Equation 56 of the dianion mechanism as previously described. It can be calculated at the initial concentration as well as at various extends of reaction. For the one case mentioned previously at [ROH] < [K⁺An⁻], an empirical fit of the data (Equations 59,58) over the first half-life of the decay curve gives the corresponding values of f(An,ROH). Finally, Equation 70 was fitted by least-squares to all the data over a wide range of values of [ROH] and [An]. The data

are given in Table III. Figure 17 allows us to judge the "goodness of fit" of the expression to the data over almost 3 orders of magnitude of the function f(An,ROH). Most of the points agree with the calculated values to within one or two standard deviations of repeated pushes. The final values obtained for the 3 parameters in Equation 70 are given in Table IVa.

The validity of this indirect method was checked in the following way: we fit all of the decay curves to Equation 70, with the 3 parameters replaced by their corresponding values from Table IVa, allowing only the initial concentration to be adjusted. Figure 18 shows some representative observed and calculated curves which were obtained in this way for varying initial conditions. The particular curves which are displayed were chosen on the basis that their deviation from the corresponding calculated curves represents about the average deviation of all of the data.

5.1.3.2--Cation Solvation Mechanism

Another hint about a possible mechanism came from the research of Fujihira and co-workers (46) who observed a pronounced effect of [H₂O] on the protonation rate of An⁻ in DMF-water mixture. This effect was interpreted by them as due to the stabilization of charge localization in the transition state by hydrogen bonding (45,66). Such an effect, if applied to our system, might increase the rate of formation of

TABLE III

Observed and Calculated Pseudo Second-Order Rate Constants for the Reaction of K⁺An⁻ with EtOH in THF and Pseudo First-Order Contribution at High Ethanol Concentrations (from this study)

-1)																	
υ	ď		1		-	ł	-	İ	-	!	! ! !	!	1	!	!	-	
Pseudo First-order Rate Constants (sec	^{بد} ا	-	!	1	!	1		-	1	!	!		-	!	-	!	
te -4)	Ω a			980.0	0.015	0.05	0.026	0.08	0.116	0.051	0.049	0.084	0.037	0.22	0.018	0.29	
d-Order Ra	f obs	0.00421 ^b	q89800°0	0.0367 ^b	0.121 ^b	1.08 ^b	0.210 ^b	1.14 ^b	0.460 ^e	0.151 ^C	0.286 ^b	0.336	0.345 ^b	1.06 ^C	0.927 ^b	1.08 ^b	
Pseudo Second-Order Rate Constants (M ⁻¹ sec ⁻¹ x10 ⁻⁴)	Ecalc (eqn.70)	0.00605	0.0121	0.0505	0.177	0.563	0.286	0.688	0.815	0.143	0.224	0.476	0.287	0.948	0.940	0.978	
	Number of Pushes	1	п	4	2	2	2	2	ю	4	ю	ю	m	4	Ŋ	2	
	[An] _o x10 ² M	4.43	4.42	4.40	1.06	0.237	1.04	0.220	0.153	4.35	2.55	0.989	2.53	0.155	0.236	0.219	
	EtOH] x10 ³ M [An ⁷] x10 ³ M	0.83	0.73	1.12	0.76	0.24	1.23	0.58	1.92	2.12	0.56	2.24	1.09	1.86	0.25	09.0	
	[EtOH] x10 3M	90.0	0.12	0.51	09.0	0.78	1.06	1.13	1.33	1.51	1.65	2.07	2.22	2.43	3.14	3.50	

!	ļ	1	!	!	0.16	1.48	0.83	0.28	0.33	8.2	12.7	
		-	!	!	0.55	3.73	1.42	3.62	6.74	53.1	53.1	
0.075	0.11	0.18	0.26	0.11	0.08	60.0	0.12	0.20	1.37	1.44	5.5	
0.462 ^C	0.604 ^C	1.18 ^c	1.85 ^d	0.995 ^d	1.83 ^d	3.52 ^d	2.54 ^d	3.56 ^d	4.70 ^d	9.48 ^d	18.4 ^d	
0.421	0.716	1.07	1.26		1.83		3.22	3.28	4.35	12.2	12.3	
ĸ	9	9	9	e	4	4	ហ	4	ĸ	9	т	7
2,46	0.998	0.166	0.062	0.833	2.46	4.39	0.160	0.199	0.062	4.42	0.238	J
2.41	2.05	1.66	0.19	0.14	1.97	1.28	1.74	0.97	0.20	06.0	0.37	
3.53	4.23	4.55	8.70	8.73	37.66	85.74	86.38	88.95	131.4	446.5	449.5	7

^aSee footnote (b) from Table V.

b Rate constants after various extents of reaction from fit of Equation 54.

^CInitial rate constants from fit of Equation 54.

drom fit of data to parallel first- and second-order decay.

enitial rate constant from empirical fit of data.

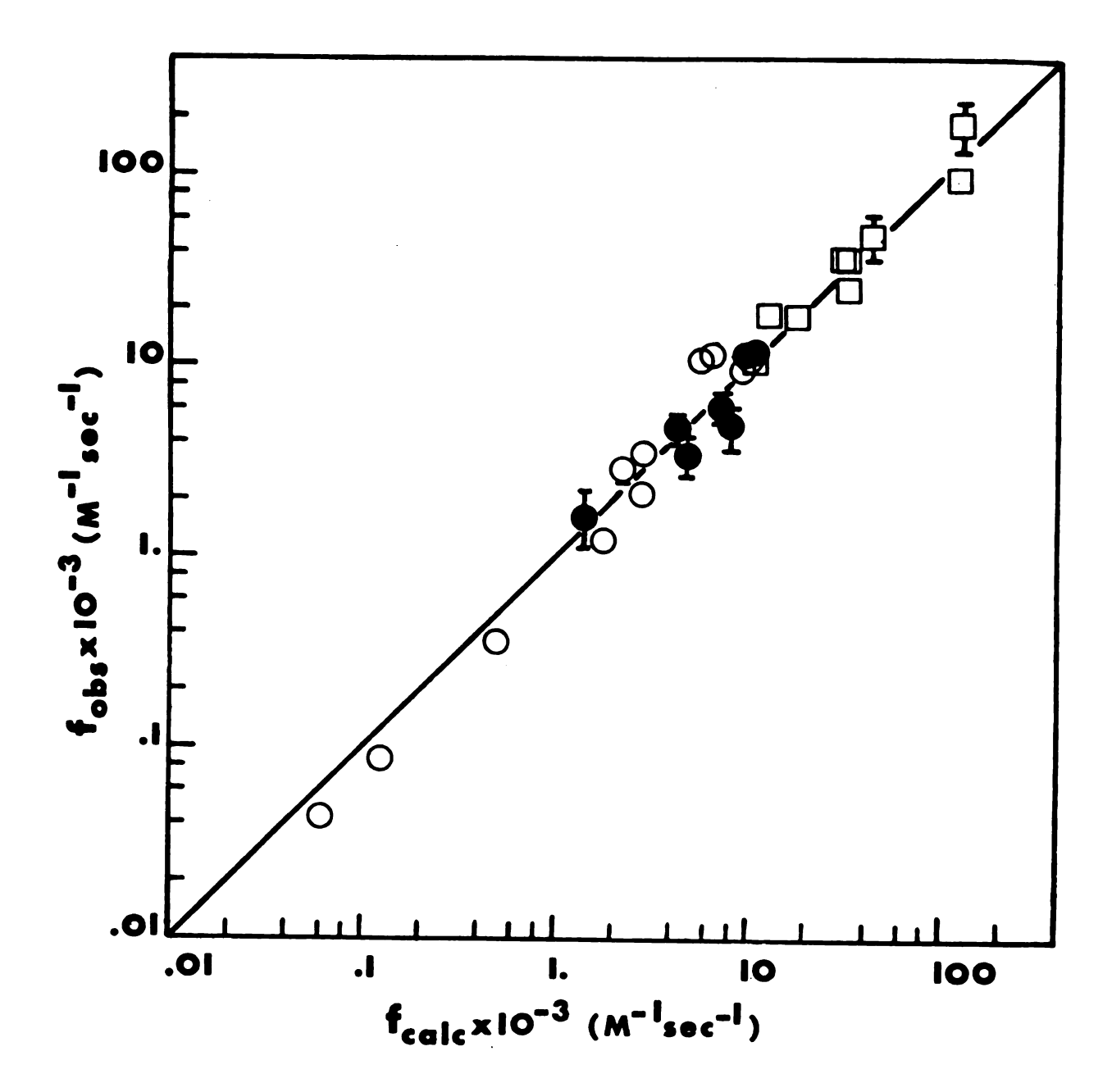
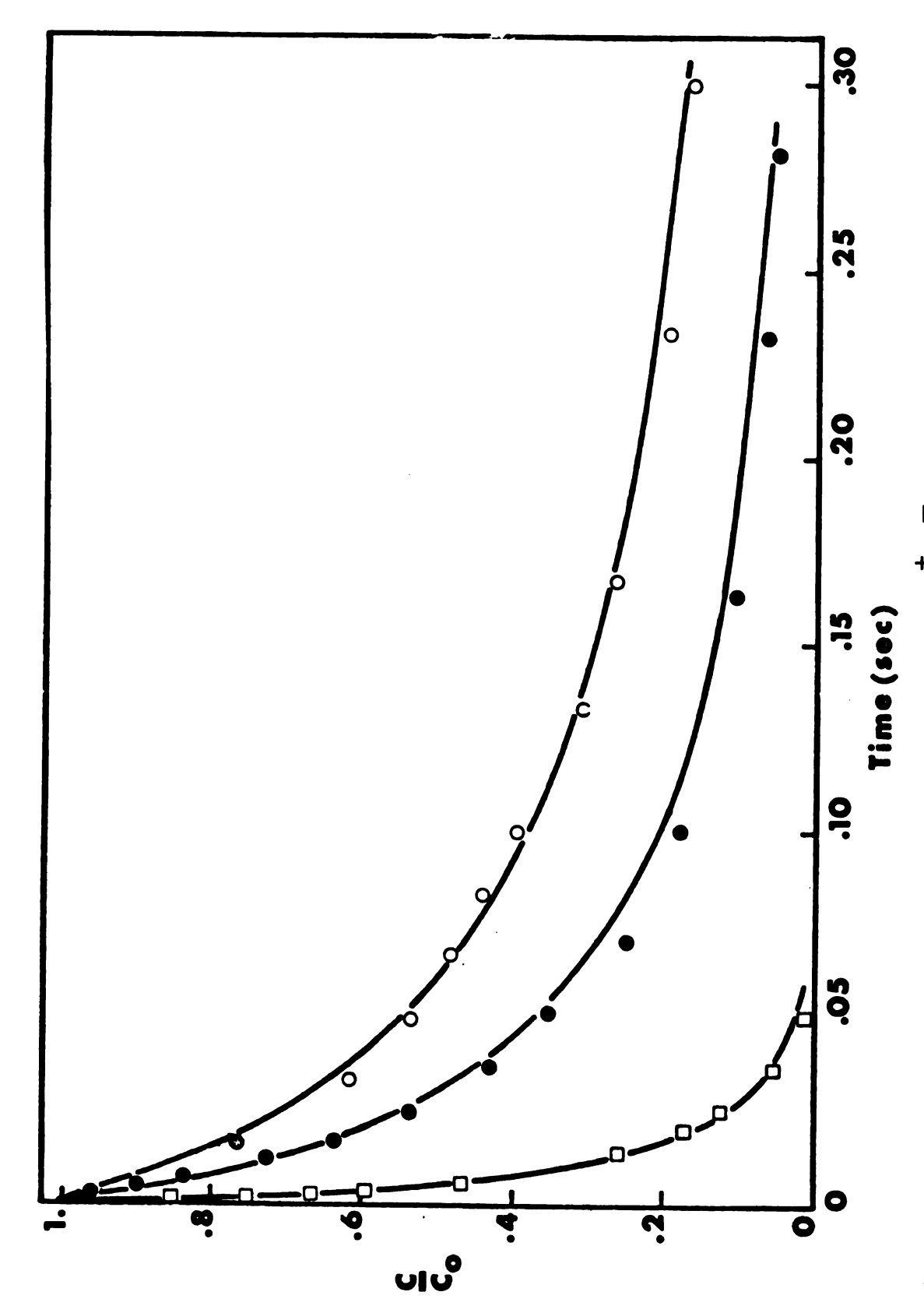


Figure 17. Log-log plot of fobs vs fcalc: (0) fobs at various extents of reaction; (1) fobs from initial rates; (1) fobs from parallel firstand second-order fit of entire decay curve.

TABLE IV

Calculated Constants from Equation (70)

	(a) with EtOH	(b) with all proton donors
$k_+^n K_Q =$	$(5.33\pm0.32) \times 10^3 \text{M}^{-1} \text{sec}^{-1}$	$(6.09\pm0.71) \times 10^3 \text{M}^{-1} \text{sec}^{-1}$
^ 1		0.35±0.14
$k_2 K_Q =$	$(1.25\pm0.07) \times 10^5 \text{M}^{-2} \text{sec}^{-1}$	$(1.33\pm0.08) \times 10^5 \text{m}^{-2} \text{sec}^{-1}$



C/C vs time for the reaction of K[†]An^{*} with EtOH in THF at three different values of [EtOH] . Solid lines (——) represent calculated curves. The constants of Equation 70 used for this calculation are given in Table IVa. Figure 18.

the anthracene dianion, or speed up the protonation rate of the ion-cluster intermediate species, because of the proximity of ROH to the aromatic anion when the ROH is complexed to K⁺. Cram and co-workers (67) proposed a "cation solvation" of ROH for proton or deuteron exchange on carbanions. According to this mechanism, the potassium cation may experience the substitution of ROH for one molecule of THF in the primary solvation layer.

$$K^+ + ROH \xrightarrow{K_S} K^+.ROH$$
 (71a)

or

$$An^{-}, K^{+} + ROH \xrightarrow{K_{S}} An^{-}, K^{+}.ROH$$
 (71b)

This cation solvation could increase the charge localization on An^T in the vicinity of the cation. If this increases the formation rate of the anthracene diamion, then one obtains the expression:

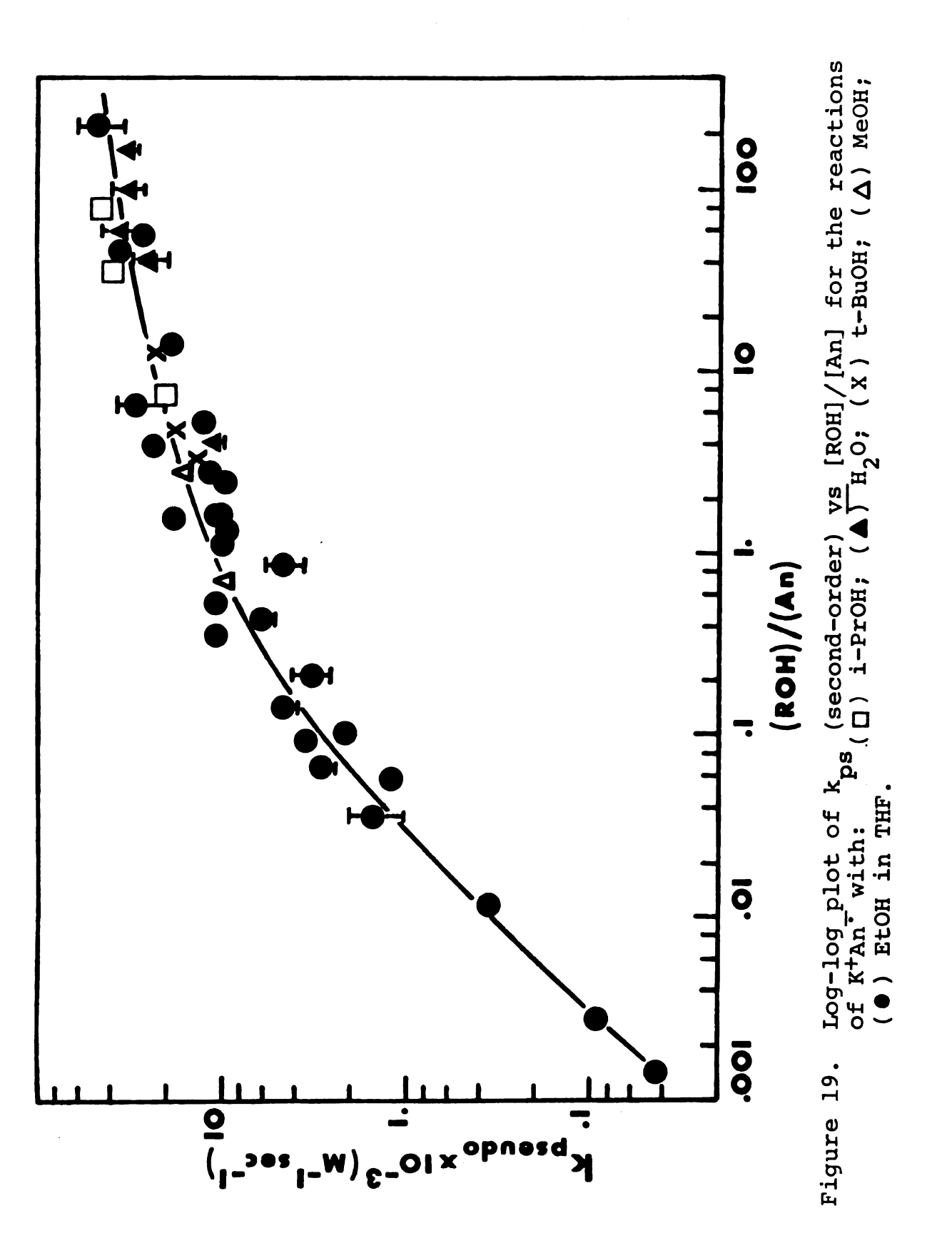
$$f(An,ROH) = (1 + K_S[ROH])^{-2} \left[\frac{2k_+ + 2K_S k_a[ROH]}{1 + \frac{k_-}{k_1} \frac{[An]}{[ROH]}} \right]$$
(72)

It is necessary to assume that the same anthracene dianion species is formed. In this expression $k_{\underline{a}}$ is the accelerated dianion formation rate constant. On the other hand, if the cation-solvation helps to increase the protonation rate of the ion-cluster, then:

$$f(An,ROH) = (1 + K_S[ROH])^{-2} \left[\frac{2k \# K_Q}{\frac{k \# [An]}{1 + \frac{k \# [ROH]}{k_1}}} + 2K_Q K_S k_2^{*}[ROH] \right]$$
(73)

Equations 70, 72 and 73 turned out to be nearly the same as far as the least-squares fitting routine is concerned, since they all contain 3 parameters, and $K_S[ROH]$ is apparently small compared to unity. This was tested by fitting the data with Equation 72. Moreover, when [ROH] is high enough to make the first-order term in [ROH] predominant, the value of the term which contains [An]/[ROH] becomes small compared to unity.

In order to try to distinguish between the various mechanisms, we used the re-analyzed data of Minnich for the protonation of K⁺An⁺ by EtOH, MeOH, i-PrOH, t-BuOH and H₂O in THF. When we used both Minnich's data and ours to test the dependence of the pseudo second-order protonation rates upon the nature of the alcohol used, we found, not without surprise, that the nature of the proton donors did not influence the protonation rate significantly. This is shown in Figure 19. We would like to emphasize here again that Minnich did not cover a wide range of concentrations of ROH and An, and, except for ethanol, the data in Figure 19 were obtained at values of [ROH] above that for which the dianion mechanism is valid. In order to include the data for ethanol on this graph, the rate constants are plotted vs [ROH]/[An] rather than [ROH] alone. However, in order to do this, the ethanol



data for which both [EtOH] and [An] were high could not be included in Figure 19. This figure shows us that all the data points fall on nearly the same curve, independent of the nature of the alcohols used. This apparent insensitivity of the protonation rate to the nature of ROH indicates that the breakdown of the dianion mechanism at high [ROH] may be due to a modified cation solvation mechanism. If we add to reactions:

$$2 (An^{-}, K^{+}) \xrightarrow{k_{+}} An^{=}, 2K^{+} + An$$
 (55a)

$$An^{-}, 2K^{+} + ROH \xrightarrow{k_{1}} K^{+}AnH^{-} + K^{+}OR^{-}$$
 (55b)

$$An^{-}, K^{+} + ROH \xrightarrow{K_{S}} An^{-}, K^{+}.ROH$$
 (71b)

the reactions which effectively yield:

$$An^{-}, K^{+} + An^{-}, K^{+}.ROH \xrightarrow{k} K^{+}AnH^{-} + K^{+}RO^{-} + An$$
 (74)

we can derive another general rate law:

$$f(An,ROH) = (1 + K_S[ROH])^{-2} \left[\frac{2k_{+}}{\frac{k_{-}[An]}{1 + \frac{k_{-}[ROH]}{[ROH]}}} + 2k_{d}K_{S}[ROH] \right]$$
(75)

The reaction described by Equation 74 might have the anthracene dianion as an intermediate species which would then be protonated by the cation-solvated alcohol K^+ ROH. Step (55b)

should be very fast (nearly diffusion controlled) in order to explain the insensitivity to the nature of ROH. Equation 75 has the same form as Equation 73. And since $K_S[ROH] << 1$ as expected, Equation 75 is similar to Equation 70 from the dianion and ion-cluster mechanism. When we used Equation 70 to fit the combined data for all proton donors in THF:

- data for EtOH only (Table III)
- Minnich's data re-analyzed (Table V)

we obtained the new values of the 3 parameters of Equation 70 shown in Table IVb. They are nearly the same as the corresponding constants in Table IVa. The goodness of fit is indicated by the standard deviation of $f_{\rm calc}/f_{\rm obs}$. With the data from Table III and the values of the 3 parameters from Table IVa, we obtained a standard deviation of $f_{\rm calc}/f_{\rm obs}$ of 0.27. When all of the data from Tables III and V are combined, and the values of the constants from Table IVb are used, we get a standard deviation of $f_{\rm calc}/f_{\rm obs}$ of 0.36. This shows once more that the nature of the proton donor did not strongly affect the rate of protonation.

5.2--Discussion

5.2.1--Comparison of the Two Proposed Mechanisms

Now that we have proposed alternate mechanisms for the reaction of K⁺An⁻ with alcohols in THF, it is in order to ask which mechanism might be preferable. The answer to this question might lie in the apparent insensitivity of the

TABLE V

Pseudo Second-order Rate Constants for the Reaction 2K An + 2ROH THF An Anh + 2K OR + An (from Minnich's re-analyzed data)

	[ROH] _o x10 ² M	[K ⁴ An ⁷] _o x10 ⁴ M	[An] _o x10 ³ M	Number of Pushes	$\frac{1}{kx}$ 10 ⁻⁴ (M ⁻¹ sec ⁻¹)	σ x10-4 (M-1 sec-1) b	1 1
Etoh	0.212 0.230 0.411 0.495	2.9 5.8 5.9	0.58 0.98 0.60 0.97	4 / 4 4	2.33 0.95 2.86 1.23	0.11 0.12 0.82 0.16	ı
н о	0.41 3.78 4.71 8.60 11.10 22.30	2.2 2.3 6.2 6.4 6.4	1.03 0.66 1.17 2.30 0.68	0 4 N N 4 N	1.13 3.50 2.49 2.37 3.26	0.18 0.91 0.57 0.23 0.51	
i-ProH	1.20 5.50 11.40	4.2 6.9 9.9	1.69 1.59 1.56	3 7	2.00 3.91 4.45	0.11 0.32 0.32	<i>3</i> 0
t-BuOH	0.54 0.80 2.03	4.7 5.3 8.8	1.69 1.70 1.59	യവയ	1.37 1.71 2.22	0.15 0.20 0.14	
меон	0.099	6,4 7,8	1,41	9 8	0.98 ^C 1.62 ^d	0,02 0,16	1

estimated standard deviation of f obtained by fitting individual decay curves is generally smaller The ^aBased upon d[An]/dt = -k[An] ². An extinction coefficient of 9.6 x 10^3 at 720 nm was used. b $0 = (\frac{1}{n-1})^2 (f_1 - (f_2))^2 (f_3)^2$ This gives a measure of the reproducibility from push to push. by a factor of 3,

^CInitial rate constant from empirical fit of data.

dgood pseudo second-order fit even though pseudo order kinetics may not be valid

protonation rate to the nature of the alcohol used especially at relatively high alcohol concentrations. If the "dianion and ion-cluster mechanism" is correct then we can reason as follows: Equation 70 derived from Equations 61 and 62, shows that at high [ROH], the second term is predominant. Since this term arises from protonation of the ion-cluster, at high values of [ROH], protonation of the ion-cluster rather than protonation of the diamion becomes the predominant pathway. On the other hand, from the estimated value $K_{\Omega} \simeq 50 \text{ M}^{-1}$ and the computed value $k_2 K_0 = 1.25 \times 10^5 M^{-2} sec^{-1}$ (Table IVa), we can estimate $k_2 \approx 2.5 \times 10^3 \text{M}^{-1} \text{sec}^{-1}$. This small value of the protonation rate constant for the ion-cluster would predict a strong influence of the acidity of the alcohols on the protonation rate. Minnich's data combined with ours (Figure 19) showed no such effect. However, in contrast, the cationsolvation mechanism provides a different picture. The proton donor is already present in the ion-cluster as K⁺.ROH. the so-called intra-complex protonation might be much faster since the interaction of ROH with K^{+} and with the negative charge on the aromatic system could very well make the alcohol more acidic. If the intra-complex protonation rate was sufficiently fast, the system need not be affected strongly by the acidity of the proton donors. Therefore, the cation solvation mechanism in combination with the dianion mechanism seems to be preferable when compared with the dianion and ion-cluster mechanism, at least at relatively high concentrations of proton donors.

5.2.2--Discrepancies Between Some of Minnich's Results and Those of Bank and Bockrath

It may be profitable to take a closer look at some apparent discrepancies which have occurred between the results obtained in this laboratory and some which have been recently published.

As described in the Historical section, Minnich (48) and Bank and Bockrath (50) independently studied the protonation of Na An with HoO in THF. While Bank and Bockrath reported only a pseudo first-order behavior of the protonation rate (first-order in the absorbance) with a rate constant $2k = 1328 \text{ M}^{-1} \text{sec}^{-1}$, Minnich found in one attempt a mixed pseudo first- and second-order behavior with a relatively large first-order contribution, and in another attempt, only a pseudo second-order decay. This inconsistency forced Minnich to eliminate this reaction from quantitative consideration. On the other hand, although the experimental details are sketchy, Bank and Bockrath reported in their experimental part (50) that considerable (up to 90% or more) decomposition of the sodium naphthalenide solution occurred in the syringe prior to data collection. This fact suggests that perhaps the pseudo first-order decay observed by Bank and Bockrath and in one of his runs by Minnich was caused by the reaction of Na An with impurities. Alternatively, impurities could catalyze the protonation reaction. If this were the case, then the reported value of the rate constant $(2k = 1328 \text{ M}^{-1} \text{sec}^{-1})$

would be larger than the true one. The reported rate constant predicts a maximum half-life of 32 msec for $[{\rm H_2O}] = 0.016$ M. At about the same water concentration, a typical push from Minnich's data for the run which showed little first-order decay, recorded successive half-lives of 180, 450 and 700 msec starting from $[{\rm Na}^+{\rm An}^-] \simeq 1.2 \times 10^{-4}$ M. However, for a typical push from the run which showed a large first-order contribution, we found successive half-lives of 26, 34 and 26 msec for $[{\rm H_2O}] = 0.047$ M. At this water concentration, Bank and Bock-rath's results predict a half life of 11 msec. Thus, it seems to us that the pseudo first-order protonation rate reported by Bank and Bockrath is too fast to be reliable. It is, of course, possible that impurities in our system inhibit the first-order reaction. The factors which accelerate or inhibit the first-order protonation deserve further study.

5.3--Summary

In summary, our results show that the disappearance of K^+An^- in its reaction with EtOH in THF is second-order in the absorbance. At low concentrations of ROH, the major protonation pathway is <u>via</u> the diamion intermediate species. At higher concentrations of ROH, the rate becomes less sensitive to the anthracene concentration while remaining largely second-order in K^+An^- . This suggests the participation of an ion-cluster $(An^-, K^+)_2$, or "solvent caged complex" (52) $(An^-, 2K^+, An)$ in the protonation process. This intermediate

might be directly protonated or it may yield a dianion species,

An =,2K + and an anthracene molecule by rapid electron-transfer

prior to the protonation step. It is likely that one of

these intermediate species can be rapidly protonated by a

cation-solvated ROH molecule (K + ROH), which is present with
in the complex.

We also found that direct protonation of the contact ionpairs An, K by ROH is slower than the second-order processes at the concentrations which we used.

The crown effect strongly indicates that the pseudo second-order pathway requires formation of contact ion-pairs. Also the pseudo first-order component obtained with the presence of crown is much smaller than the corresponding one obtained without crown.

5.4--Conclusion and Suggestions for Further Work

In the concluding part of this work, we would like to present a general picture of the protonation reaction of aromatic radical anions with alcohols, by combining our results with the results found in the recent literature. This general view is that the protonation rate depends not only upon the acidity of the proton donor, but also on the degree of charge localization in the aromatic system. We expect the charge localization to decrease in the following order:

- 1) dianion $(An^{=}, 2M^{+})$
- 2) ion-cluster (An,M,)

- 3) contact ion-pair (An,M+)
- 4) solvent-separated ion-pair (An | M)
- 5) free or solvent solvated ion (AnT).

Let us denote the protonation rate constants (with EtOH) of these species by k_1 , k_2 , ... k_5 , respectively. The results obtained in DMF as solvent (45) give $k_5 \approx 2 \times 10^{-4} \text{M}^{-1} \text{sec}^{-1}$. Our result for K^+An^- with crown in THF allows an estimation of $k_4 \approx 2 \text{M}^{-1} \text{sec}^{-1}$. The data of Rainis, Tung and Szwarc (52) for DME as solvent give $k_4 \approx 6 \text{M}^{-1} \text{sec}^{-1}$ (provided that we assume that Na^+An^- exists in DME largely as the solvent-separated ion-pair). From our data, $k_3 \approx 200 \text{ M}^{-1} \text{sec}^{-1}$ at high values of [EtOH] but we are not sure that the direct protonation reactions are even bimolecular. The protonating agents may well exist under aggregated forms (ROH) (46,52).

An estimation of the value of k_2 is somewhat more complicated, since it depends upon the nature of the protonated species. The ion-cluster $(An^{-},K^{+})_2$ may transform to $(An^{-},2K^{+},An)$, the "solvent caged complex" (52) prior to protonation. In this case, the protonation rate constant k_2 is expected to be near the diffusion controlled limit. On the other hand, if the protonated species is the ion-cluster itself, then $k_2 \approx 2.5 \times 10^3 M^{-1} sec^{-1}$ (section 5.2.1).

Finally, Table IVa gives $\frac{k_{-}}{k_{1}} \cong 0.3$, and k_{+} (or $k_{+}^{"}K_{Q}$) \cong $5 \times 10^{3} \text{M}^{-1} \text{sec}^{-1}$. Potentiometric data (68) yield a value of about 1×10^{-5} for the overall disproportionation equilibrium constant for the reaction:

$$2 (An^{-}, K^{+}) \xrightarrow{k_{+}} An^{=}, 2K^{+} + An$$
 (55a)

in THF. Thus k_ (or k_") \approx 5 x 10⁸ M⁻¹sec⁻¹. Hence k₁ \approx 1.5 x 10⁹ M⁻¹sec⁻¹.

From all the values of the protonation rate constants obtained above, we can see that the order $k_1 >> k_2 > k_3 > k_4 > k_5$ agrees well with the degree of charge localization in the aromatic system:

$$(An^{-}, 2M^{+}) > (An^{-}, M^{+})_{2} > (An^{-}, M^{+}) > (An^{-} | | M^{+}) > (An^{-})$$

For further work in this area, we would like to propose a careful and extensive study of the system Na⁺An⁻ with H₂O in THF in order to clarify the discrepancies between the results of Minnich on one hand and those of Bank and Bockrath on the other hand. Also, in order to obtain a better understanding of the "solvent effect", a study of one system over the entire range of solvent composition would be very interesting. The system DMF-ethanol would be appropriate since only the first-order process was observed (46). Pulseradiolysis techniques, the stopped-flow method and conventional studies would be required to cover the high, intermediate and low ethanol concentration cases.

REFERENCES

- 1. W. Schlenk, J. Appenrodt, A. Michael, and A. Thal, Chem. Ber., 47, 479 (1914).
- N. D. Scott, J. F. Walker, and V. L. Hansley, J. Amer. Chem. Soc., 58, 2442 (1936).
- 3. D. E. Paul, D. Lipkin, and S. I. Weissman, <u>J. Amer. Chem. Soc.</u>, 78, 116 (1956).
- P. Balk, G. J. Hoijtink, and J. W. H. Schreurs, <u>Rec. Trav. Chim.</u>, 76, 813 (1957).
- 5. E. DeBoer, and S. I. Weissman, <u>Rec. Trav. Chim.</u>, <u>76</u>, 824 (1957).
- 6. G. J. Hoijtink and P. J. Zandstra, Mol. Phys., 3, 371 (1960).
- 7. K. H. J. Buschow, J. Dieleman, and G. J. Hoijtink, Mol. Phys., 7, 1 (1963-64).
- 8. H. A. Laitinen, and S. Wawzonek, <u>J. Amer. Chem. Soc.</u>, 64, 1765 (1942).
- 9. A. Maccoll, <u>Nature</u>, <u>163</u>, 178 (1949).
- 10. G. J. Hoijtink, and J. Van Schooten, Rec. Trav. Chim., 71, 1089 (1952).
- 11. G. J. Hoijtink, J. Van Schooten, E. DeBoer, and W. Ij. Aalbersberg, Rec. Trav. Chim., 73, 355 (1954).
- 12. G. J. Hoijtink, E. DeBoer, P. H. Van Der Meij, and W. P. Weijland, Rec. Trav. Chim., 75, 487 (1956).
- 13. T. L. Chu and S. C. Yu, <u>J. Amer. Chem. Soc.</u>, <u>76</u>, 3367 (1954).
- 14. T. R. Tuttle, Jr., R. L. Ward, and S. I. Weissman, J. Chem. Phys., 25, 189 (1956).

- 15. E. DeBoer, J. Chem. Phys., 25, 190 (1956).
- 16. E. DeBoer, and S. I. Weissman, <u>J. Amer. Chem. Soc.</u>, <u>80</u>, 4549 (1958).
- 17. R. L. Ward, and S. I. Weissman, <u>J. Amer. Chem. Soc.</u>, 79, 2086 (1957).
- 18. N. M. Atherton, and S. I. Weissman, <u>J. Amer. Chem. Soc.</u>, 83, 1330 (1961).
- K. H. J. Buschow, J. Dieleman, and G. J. Hoijtink,
 J. Chem. Phys., 42, 1993 (1965).
- 20. A. Crowley, N. Hirota, and R. Kreilick, <u>J. Chem. Phys.</u>, 46, 4815 (1967).
- 21. C. L. Dodson and A. H. Reddoch, <u>J. Chem. Phys.</u>, <u>48</u>, 3226 (1968).
- 22. R. V. Slates, and M. Szwarc, <u>J. Phys. Chem.</u>, <u>69</u>, 4124 (1965).
- 23. T. E. Hogen-Esch, and J. Smid, <u>J. Amer. Chem. Soc.</u>, <u>88</u>, 307 (1966).
- 24. P. Biloen, T. Fransen, A. Tulp, and G. J. Hoijtink, J. Phys. Chem., 73, 1581 (1969).
- 25. N. Hirota, R. Carraway, and W. Schook, <u>J. Amer. Chem. Soc.</u>, 90, 3611 (1968).
- 26. T. E. Hogen-Esch, and J. Smid, <u>J. Amer. Chem. Soc.</u>, <u>88</u>, 318 (1966).
- 27. N. Hirota, <u>J. Amer. Chem. Soc.</u>, <u>90</u>, 3603 (1968).
- 28. P. Chang, R. V. Slates, and M. Szwarc, <u>J. Phys. Chem.</u>, 70, 3180 (1966).
- 29. W. Schlenk, and E. Bergman, Ann., 463, 134 (1928).
- 30. W. E. Bachman, J. Org. Chem., 1, 347 (1936).
- 31. J. F. Walker and N. D. Scott, <u>J. Amer. Chem. Soc.</u>, <u>60</u>, 951 (1938).
- 32. A. P. Krapcho, and A. A. Bothner-By, <u>J. Amer. Chem. Soc.</u>, <u>81</u>, 3658 (1959).

- 33. A. P. Krapcho, and A. A. Bothner-By, <u>J. Amer. Chem. Soc.</u>, 82, 751 (1960).
- 34. O. J. Jacobus, and J. F. Eastham, <u>J. Amer. Chem. Soc.</u>, 87, 5799 (1965).
- 35. E. J. Kelly, H. V. Secor, C. W. Keenan and J. F. Eastham, J. Amer. Chem. Soc., 84, 3611 (1962).
- 36. W. L. Jolly, "Solvated Electron", Advances in Chemistry Series No. 50, American Chemical Society, Washington, D. C. (1965).
- 37. A. M. Kahn, and R. R. Dewald, Proceedings of Colloque Weyl III, Hanita, Israel, June 1972 (in press).
- 38. J. P. Keene, E. J. Land, and A. J. Swallow, <u>J. Amer.</u> Chem. Soc., 87, 5284 (1965).
- 39. S. Arai, and L. M. Dorfman, <u>J. Chem. Phys.</u>, <u>41</u>, 2190 (1964).
- 40. L. M. Dorfman, Acc. Chem. Res., 3, 224 (1970).
- 41. S. Arai, and L. M. Dorfman, <u>J. Phys. Chem.</u>, <u>69</u>, 2239 (1965).
- 42. J. R. Brandon, and L. M. Dorfman, <u>J. Chem. Phys.</u>, <u>53</u>, 3849 (1970).
- 43. K. Umemoto, Bull. Chem. Soc. Jap., 40, 1058 (1967).
- 44. S. Hayano and M. Fujihira, <u>Bull. Chem. Soc. Jap.</u>, <u>44</u>, 1496 (1971).
- 45. S. Hayano, and M. Fujihira, <u>Bull. Chem. Soc. Jap.</u>, <u>44</u>, 2046 (1971).
- 46. M. Fujihira, H. Suzuki, and S. Hayano, J. Electro. Anal. Chem., 33, 393 (1971).
- 47. E. R. Minnich, and J. L. Dye, Abstracts, 161st National Meeting of the American Chemical Society, Los Angeles, California, March 1971.
- 48. E. R. Minnich, Ph. D. thesis, Michigan State University, (1970).
- 49. S. Bank, and B. Bockrath, <u>J. Amer. Chem. Soc.</u>, <u>93</u>, 430 (1971).

- 50. S. Bank, and B. Bockrath, <u>J. Amer. Chem. Soc.</u>, <u>94</u>, 6076 (1972).
- 51. G. Levin, C. Sutphen, and M. Szwarc, <u>J. Amer. Chem. Soc.</u>, 94, 2652 (1972).
- 52. A. Rainis, R. Tung, and M. Szwarc, private communication. To be published in J. Amer. Chem. Soc.
- 53. E. R. Minnich, L. D. Long, J. Ceraso, and J. L. Dye, to be published in J. Amer. Chem. Soc.
- 54. E. M. Hansen, Ph. D. thesis, Michigan State University (1970).
- 55. L. H. Feldman, Ph. D. thesis, Michigan State University (1966).
- 56. M. G. DeBacker, Ph. D. thesis, Michigan State University (1970).
- 57. J. L. Dye, and V. A. Nicely, <u>J. Chem. Ed.</u>, <u>48</u>, 443 (1971).
- 58. V. A. Nicely, Ph. D. thesis, Michigan State University (1969).
- 59. C. J. Pedersen, J. Amer. Chem. Soc., 89, 7017 (1967).
- 60. J. L. Dye, M. T. Lok, F. J. Tehan, R. B. Coolen, N. Papadakis, J. M. Ceraso, and M. DeBacker, Ber. Bunsen Gesell. Phys. Chem., 75, 659 (1971).
- 61. K. H. Wong, G. Konizer, and J. Smid, <u>J. Amer. Chem. Soc.</u>, 92, 666 (1970).
- 62. R. M. Fuoss, and C. A. Kraus, <u>J. Amer. Chem. Soc.</u>, <u>57</u>, 1 (1935).
- 63. R. M. Fuoss, J. Amer. Chem. Soc., 80, 5059 (1958).
- 64. M. Szwarc, "Carbanions, Living Polymers and Electron-Transfer Processes", Interscience, New York, 1968.
- 65. R. M. Fuoss and C. A. Kraus, <u>J. Amer. Chem. Soc.</u>, <u>55</u>, 2387 (1933).
- 66. S. Hayano, and M. Fujihira, <u>Bull. Chem. Soc. Jap.</u>, <u>44</u>, 2051 (1971).
- 67. S. M. Wong, H. P. Fisher, and D. J. Cram, <u>J. Amer. Chem.</u> Soc., <u>93</u>, 2235 (1971).

68. J. Jagur-Grodzinski, M. Feld, S. L. Yang and M. Szwarc, J. Phys. Chem., 69, 628 (1965).

